HHS Public Access

Author manuscript

Sci Immunol. Author manuscript; available in PMC 2022 January 02.

Published in final edited form as:

Sci Immunol. 2021 July 02; 6(61): . doi:10.1126/sciimmunol.abd1287.

The m^{6}A reader IMP2 directs autoimmune inflammation through an IL-17- and TNFα-dependent C/EBP transcription factor axis

Rami Bechara[1], **Nilesh Amatya**[1], **Rachel D. Bailey**[1], **Yang Li**[1], **Felix EY Aggor**[1], **De-Dong Li**[1], **Chetan V. Jawale**[1], **Bianca M. Coleman**[1], **Ning Dai**[2], **Nandan S. Gokhale**[3], **Tiffany C. Taylor**[1], **Stacy M. Horner**[3,4], **Amanda C. Poholek**[5], **Anita Bansal**[6], **Partha S. Biswas**[1], **Sarah L. Gaffen**[1,‡]

[1]Division of Rheumatology & Clinical Immunology, University of Pittsburgh, Pittsburgh, PA, USA

[2]Diabetes Unit, Massachusetts General Hospital, Boston, MA, USA

[3]Department of Molecular Genetics and Microbiology, Duke University Medical Center, Durham, NC, USA

[4]Department of Medicine, Duke University Medical Center, Durham, NC, USA

[5]Division of Pediatrics, University of Pittsburgh, Pittsburgh, PA, USA.

[6]Department of Immunology, University of Pittsburgh, Pittsburgh, PA, USA.

Abstract

Excessive cytokine activity underlies many autoimmune conditions, particularly through the IL-17 and TNFα signaling axes. Both cytokines activate NF-κB, but appropriate induction of downstream effector genes requires coordinated activation of other transcription factors, notably CCAAT/Enhancer Binding Proteins (C/EBPs). Here we demonstrate the unexpected involvement of a post-transcriptional 'epitranscriptomic' mRNA modification (N6-methyladenosine, m^{6}A) in regulating C/EBPβ and C/EBPδ in response to IL-17A, as well as IL-17F and TNFα. Prompted by the observation that C/EBPβ/δ-encoding transcripts contain m^{6}A consensus sites, we show that *Cebpd* and *Cebpb* mRNAs are subject to m^{6}A modification. Induction of C/EBPs is enhanced by an m^{6}A methylase 'writer' and suppressed by a demethylase 'eraser.' The only m^{6}A 'reader' found to be involved in this pathway was IGF2BP2 (IMP2), and IMP2 occupancy of *Cebpd* and *Cebpb* mRNA was enhanced by m^{6}A modification. IMP2 facilitated IL-17-mediated *Cebpd* mRNA stabilization and promoted translation of C/EBPβ/δ in response to IL-17A, IL-17F and TNFα. RNASeq revealed transcriptome-wide IL-17-induced transcripts that are IMP2-influenced, and RIPSeq identified the subset of mRNAs that are directly occupied by IMP2, which included *Cebpb* and *Cebpd.* Lipocalin-2 (*Lcn2*), a hallmark of autoimmune

‡Correspondence: BST S702, 200 Lothrop St., Pittsburgh PA 15261. 412-383-8903. Sarah.gaffen@pitt.edu.

Author contributions: Conceptualization: RB, NA, PSB, SLG; Methodology: NA, RB, PSB, ND, NG, ACP, AB; Investigation: RB, NA, RDB, DL, CVJ, FEYA, YL, BMC, NG, ACP, TCT, PSB, AB; Writing – Original Draft: NA, RB, SLG; Writing – Review & Editing: RB, PSB, NG, ACP, SMH, SLG; Funding Acquisition: SLG; Resources: ND, SMH; Supervision: SLG, PSB

Competing Interests: The authors declare no competing interests.

Data and Materials Availability: The RNASeq and RIPSeq data are available through the NCBI GEO resource under accession number GSE178710. Mutant mouse strains used in this study are available by MTA (*Act1*$^{-/-}$, NIH; *Il17ra*$^{-/-}$, Amgen; *Imp2*$^{-/-}$, Oxford University). All other data needed to evaluate the conclusions in the paper are present in the paper or the Supplementary Materials.

kidney injury, was strongly dependent on IL-17, IMP2 and C/EBPβ/δ. Indeed, *Imp2*$^{-/-}$ mice were resistant to autoantibody-induced glomerulonephritis (AGN), showing impaired renal expression of C/EBPs and *Lcn2*. Moreover, IMP2 deletion initiated only after AGN onset ameliorated disease. Thus, post-transcriptional regulation of C/EBPs through m^{6}A/IMP2 represents a new paradigm of cytokine-driven autoimmune inflammation.

One sentence summary:

The m6A 'reader' IMP2 promotes cytokine-induced kidney autoimmunity by posttranscriptional control of C/EBPβ/δ transcription factors.

INTRODUCTION

Over 20 million Americans live with an autoimmune disorder. The estimated economic burden in medical expenses and loss of productivity is enormous, exceeding even cancer care (1, 2). The advent of anti-cytokine antibody drugs three decades ago revolutionized treatment of many autoimmune conditions, beginning with biologics targeting TNF. More recently, IL-17 (IL-17A) and Th17 cells were found to be dysregulated in skin and joint conditions such as psoriasis, psoriatic arthritis and ankylosing spondylitis. IL-17 is also implicated in other autoimmune settings such as multiple sclerosis and autoantibody-induced glomerulonephritis (AGN) (3). In principle, understanding the molecular basis of cytokine-induced autoimmune pathology has potential to inform new therapeutic targets (4).

IL-17 signaling occurs predominantly in non-hematopoietic cell types expressing the IL-17 receptor (5), while nearly all cells express TNF receptors and are responsive to this cytokine. TNFα and IL-17 mediate many overlapping signals, leading to similar, though not identical, downstream gene profiles. Many transcription factors (TF) are activated by one or both of these cytokines, including NF-κB, IκBξ, AP-1, as well as the CCAAT/enhancer binding proteins (C/EBPs). Most known cytokine-induced genes are regulated by combinations of these TFs (6-12).

C/EBPs are leucine zipper TFs described in the 1980's, yet their regulation remains surprisingly poorly understood, especially compared to other immune TF families such as NF-κB or STATs (13-17). C/EBPs bind to characteristic motifs on target promoters and enhancers and are pleiotropic activators of inflammation in response to numerous immune and microbial stimuli (14). C/EBPs form heterodimers and homodimers and autoregulate their own promoters (14, 16). C/EBPβ exists in multiple, alternatively translated isoforms, and is also subject to inducible phosphorylation that tunes its activity in response to cytokine signals (18-22). Early studies of IL-17 showed that this cytokine induces both C/EBPδ and C/EBPβ, and both are required for induction of downstream effector genes that underlie IL-17 biologic activity (7, 8).

Whereas TNF is a potent activator of new transcription (23), IL-17 is a major activator of post-transcriptional events through a complex network of RNA binding proteins (RBPs) (5). RBPs bind to respective client transcripts at cis-acting elements typically found within 3' or 5' untranslated regions (UTRs). A variety of RBPs (Regnase-1, Arid5a, ASF/SF2,

HuR, DDX3X, Roquins, Act1) influence downstream RNA stability and/or translation in response to IL-17 (13, 24, 25). Moreover, there is crosstalk between transcriptional and post-transcriptional events, since several mRNAs encoding TFs are subject to post-transcriptional control. This phenomenon is well described for *Nfkbiz* (encoding the noncanonical NF-κB protein IκBξ) (5, 17, 26) which is regulated by Regnase-1, Arid5a and an Act1/DDX3X complex (26, 27). We recently showed that C/EBPβ, but not C/EBPδ, is regulated in part by Arid5a at the level of translation in the IL-17 pathway (17). Thus, regulation of gene expression by IL-17 and related cytokines involves transcriptional and post-transcriptional circuitry.

An underappreciated determinant of RNA fate is 'epitranscriptomic' modification of mRNA (28). N6-methyladenosine (m^6A) is added to specific RNAs by methyltransferase enzymes termed 'writers', which can be reversed by demethylases ('erasers') (29). The consequences of m^6A modification are myriad, impacting RNA stabilization, translational efficiency, splicing, nuclear export and phase separation (29). Deletion of the writer METTL3 in T cells disrupts homeostatic expansion and Treg function (30, 31), and viral infections alter m^6A modification of host gene expression (32-34). Diverse 'readers' bind to m^6A directly or to sequence structures influenced by this modification. The best-known m^6A readers belong to the YTH-domain family, which typically destabilize their respective client mRNAs. Recent work identified members of the IGF2 mRNA binding protein (IGF2BP) family (known as IMPs) as noncanonical m^6A readers that can stabilize target transcripts (35, 36). To date, the m^6A pathway has been somewhat overlooked in the immune system (37).

AGN encompasses a heterogenous group of nephritic conditions caused by inappropriate responses to renal autoantigens. The most severe form is characterized by formation of glomerular crescents and tubulointerstitial inflammation (38-40). In humans, treatment with corticosteroids and cyclophosphamide increases AGN survival somewhat, but there is an unmet need to understand events within the kidney to develop better treatment strategies (41). While traditionally considered to be a B-cell-dependent disease, T helper (Th) cells drive renal damage in AGN (42, 43). Tissue-resident memory Th17 cells specific for commensal microbes are overrepresented in human GN nephrectomy samples (44). In mice, these $T_{RM}17$ cells exacerbate pathology in crescentic GN, which was blocked with anti-cytokine antibodies that inhibit Th17 cell development (44). Lipocalin-2 (Lcn2, 24p3, NGAL) is a biomarker and driver of AGN (7, 45-47) and is potently induced by IL-17 through activation of C/EBPβ and C/EBPδ (6, 19, 26). The present study was prompted by the observation that noncoding sequences in *Cebpd* and *Cebpb* contain consensus m^6A sites. Indeed, we show that C/EBP mRNAs are subject to m^6A modification and are bound to and regulated by IMP2 (35, 48). *Imp2*$^{-/-}$ mice were resistant to AGN, and loss of IMP2 after induction of AGN ameliorated renal inflammation. Thus, induction of autoimmune nephritis is controlled by an IMP2/m^6A epitranscriptomic axis through C/EBP transcription factors.

RESULTS

Cebpd and Cebpb mRNAs are subject to m^6A modification

Prototypical genes in the IL-17 target gene signature include *Il6, Lcn2* as well as the TFs *Cebpd* and *Cebpb*, but regulation of C/EBPs has long been enigmatic. Induction of

these mRNAs is seen in numerous cell backgrounds including primary mouse embryonic fibroblasts (MEFs) and human renal epithelial cells (HK-2 (49)) (Fig 1A, fig S1a, b). The proximal promoters of the *Il6* and *Lcn2* genes contain C/EBP binding elements that are nonredundant for IL-17-dependent activation (6, 7, 19), and knockdown of C/EBPβ and C/EBPδ by siRNA in MEFs abrogated the upregulation of *Il6* and *Lcn2* by IL-17 as well as regulating one another (Fig 1A, fig S1c). As expected, IL-17 did not activate a *Lcn2* promoter with a C/EBP binding site mutation (fig S1d, e) (6). Although C/EBPs were reported to be regulated by NF-κB in response to LPS (50), an IKK inhibitor surprisingly had no impact on induction of *Cebpb* or *Cebpd* in response to IL-17, though it abolished expression of *Il6* and *Lcn2*, as expected (fig S1f) (6, 7, 51).

To gain insight into how C/EBPs are regulated in the IL-17 pathway, we examined the noncoding sequences of these intronless genes. According to the RMBase and SRAMP databases (52, 53) *Cebpd* and *Cebpb* mRNAs contain several high confidence sites of predicted or empirical N6-methyladenosine (m^6A) modification, mainly in the 3' UTR. In contrast, *Ccl20*, another mRNA induced by IL-17, contains very few predicted m^6A sites (fig S2, table S1). In general, deposition of m^6A is mediated by the methyltransferase-like 3 (METTL3) enzyme and can be reversed by demethylases such as α-ketoglutarate-dependent dioxygenase (fat mass and obesity associated protein, FTO) (28) (Fig 1B). In response to IL-17, knockdown of *Mettl3* suppressed expression of *Cebpd* mRNA (Fig 1C) as well as C/EBPδ protein (Fig 1E, F). *Mettl3* silencing also showed a trend of reduced C/EBPβ protein expression (Fig 1E, F). Correspondingly, *Mettl3* knockdown suppressed expression of the C/EBPβ/δ-dependent mRNAs *Il6* and *Lcn2*, but had no effect on *Ccl20* (fig S3). Conversely, knockdown of *Fto*, an m^6A 'eraser,' increased *Cebpd* (Fig 1D) and corresponding C/EBPδ protein levels (Fig 1G, H), and increased *Il6* and *Lcn2* levels (fig S3). Interestingly, knockdown of *Fto* only reproducibly impacted the LIP isoform of C/EBPβ, perhaps indicating selective regulation of this TF at the level of alternative translation (Fig 1G, H). These data indicate involvement of the m^6A pathway in control of C/EBPs.

To determine if C/EBP mRNAs are subject to m^6A modification, we performed RNA immunoprecipitation (RIP) with anti-m^6A antibodies (32). There was no enrichment of *Cebpd* or *Cebpb* in control IgG RIP samples (Fig 1I). Likewise, *Ccl20* was not detected in m^6A RIP samples, commensurate with its lack of predicted m^6A motifs (fig S2, table S1). However, *Cebpd* mRNA was substantially increased upon anti-m^6A RIP, both at baseline and after IL-17 treatment (Fig 1I). *Cebpb* mRNA was also constitutively enriched in anti-m^6A RIPs, and did not change upon IL-17 signaling (Fig 1I). These data therefore implicate the m^6A pathway in regulation of C/EBPs, and consequently the expression of downstream target mRNAs.

The m^6A reader IMP2 promotes expression of IL-17 target genes via C/EBPs

Given this evidence that the m^6A machinery regulates IL-17-dependent gene expression, we sought to define possible m^6A RNA binding proteins ('readers') required for this process. Surprisingly, knockdown of none of the canonical YTH m^6A readers suppressed *Il6, Lcn2* or *Cebpd* (though knockdown of *Ythdf1* increased *Cebpd* expression, suggesting it may be

a negative regulator) (Fig 2A, fig S4). We noted that the predicted m^{6}A motifs in *Cebpd* and *Cebpb* corresponded closely to consensus recognition sites for the noncanonical m^{6}A readers of the IGF2BP family (known as IMPs), recently shown to stabilize client mRNAs such as *Myc* (35, 54). In MEFs, only IMP2 was expressed at substantial levels. To determine if IMP2 participates in the IL-17 pathway, MEFs were transfected with siRNA targeting *Imp2*, treated with IL-17 for 8 h, and subjected to RNA-Seq and Ingenuity Pathway Analysis (IPA). The top upstream regulators identified by IPA to be IMP2-dependent were TRAF3IP2 (better known as the IL-17-associated adaptor Act1) and IL-17A, as well as closely related pathways including TNFα, LPS, IL-1 family and NF-κB (fig S5a). Strikingly, following *Imp2* knockdown, all these pathways were abrogated (Fig 2C).

Consistent with this, many characteristic IL-17 signature genes were reduced upon IMP2 knockdown, including *Il6, Lcn2, Cebpd* and several chemokines (*Cxcl1, Cxcl5, Ccl2, Ccl7*). (Fig 2C, fig S5b-e). Expression of selected genes was verified by qPCR (Fig 2D). Importantly, not all IL-17-induced genes were impacted by IMP2 deficiency such as *Ccl20,* revealing a level of specificity in the genes controlled by IMP2 (Fig 2D, fig S5e). This was consistent with absence of *Ccl20* in m^{6}A RIP samples (Fig 1I). Further supporting these findings, MEFs derived from *Imp2*$^{-/-}$ mice showed impaired IL-17 induction of *Il6* and *Lcn2* but not *Ccl20* (Fig 2E). Also consistent with this, IMP2 was required for IL-17-induced expression of *IL6* and *LCN2* in HK-2 cells, a human renal epithelial cell line (Fig 2F). IMP2 knockdown did not alter expression of proximal signaling intermediates in the IL-17 pathway such as *Il17ra, Act 1 (Traf3ip2), Traf2* or *Traf6*, (fig S5e, f), nor did loss of IMP2 affect expression of any m^{6}A readers/writers/erasers tested (fig S5e, g). Based on IPA predictions (Fig 2C), we evaluated the role of IMP2 in related cytokine pathways. IMP2 deficiency led to reduced IL-17F- and TNFα-mediated upregulation of *Il6* and *Lcn2* (fig S5h), indicating that the IMP2 pathway is applicable to analogous cytokine pathways.

We next tested the hypothesis that IMP2 controls these downstream genes through regulation of C/EBPs. In MEFs and HK-2 cells, C/EBPδ mRNA and protein were elevated in response to IL-17 in an IMP2-dependent manner, demonstrated by siRNA and in *Imp2*$^{-/-}$ cells (Fig 3A-C, F, fig S6a). Unlike C/EBPδ, IMP2 deficiency did not impair *Cebpb* mRNA expression (Fig 3A, B), but protein levels of C/EBPβ were reduced in *Imp2*$^{-/-}$ cells or following *Imp2* silencing. C/EBPβ has three major isoforms generated by alternative translation, LAP*, LAP, LIP; while all were impaired to some degree, LIP appeared to be the most sensitive to IMP2 deficiency (16) (Fig 3C, F, G, fig S6a-d). Likewise, C/EBPδ and C/EBPβ proteins were elevated in response to IL-17F in an IMP2-dependent manner (fig S6e). While TNFα-induced C/EBPβ protein was similarly IMP2-dependent (Fig 3E), TNFα did not induce C/EBPδ protein even at high concentrations, revealing a distinction between the transcription factors induced by IL-17 family cytokines compared to TNFα (Fig 3D).

Next, we assessed the impact of IMP2 deficiency on activation of promoters that require C/EBP binding sites for IL-17/TNFα-mediated induction (6, 7). As shown, induction of a Luciferase (Luc) reporter driven by the *Il6* or *Lcn2* proximal promoters was largely abrogated in *Imp2*$^{-/-}$ MEFs (Fig 3H, fig S7a). Activation of the *Il6* or *Lcn2* promoters in *Imp2*$^{-/-}$ MEFs could be rescued by ectopic expression of C/EBPδ or C/EBPβ (Fig 3I, fig

S7b, c). Together, these data support a role for IMP2 in mediating IL-17 signaling through regulation of C/EBPs.

IMP2 binds Cebpd and Cebpb mRNAs

We next evaluated the binding of IMP2 to selected IL-17-induced transcripts by RIP. Indeed, IMP2 RIP samples contained marked enrichment of both *Cebpd* and *Cebpb* mRNA compared to IgG controls, indicating that both transcripts interact directly with IMP2 (Fig 4A). Additionally, IMP2 bound to *Ccl7* quite strongly. *Il6, Lcn2* and *Cxcl1* were also enriched in IMP2 RIP samples, albeit more weakly, and there was no enrichment of *Ccl20*.

To gain a transcriptome-wide view of the IMP2 clients in the IL-17 pathway, cells were stimulated with IL-17 for 3 h and lysates subjected to RIPSeq with anti-IMP2 Abs or IgG. Results analyzed with Piranha and DESeq2 (55, 56), eliminating non-annotated regions from consideration and using a cutoff of FDR>0.01 and a 2-fold enrichment. We identified 4933 mRNAs with IMP2-interactions. In this analysis we only considered mRNAs with known IMP2 binding motifs, which constituted ~63% of the transcripts in the IMP2-RIP samples (3217 total) (57). Comparison of the RIPSeq and RNASeq datasets distinguished those mRNAs that are direct IMP2 clients (based on RIPSeq) from the entirety of transcripts that are influenced by IMP2 silencing (based on RNASeq) (Fig 4B, Fig S8B). IMP2-bound RNAs identified in RIPSeq included *Cebpd, Ccl7,* and *Il6,* thus independently confirming the validity of these mRNAs as authentic IMP2 clients (Fig 4B). *Cebpb* was also enriched in the RIPSeq dataset, but its abundance was not altered by IMP2 silencing (Fig 1, Fig 4B) (58). Also as expected, there were no detectable interactions between IMP2 and *Ccl20*, which is upregulated by IL-17 but is neither methylated nor IMP2-dependent. Unexpectedly, *Lcn2* was not enriched in the RIPSeq samples, possibly due to its relatively weak association with IMP2 seen in RIP (Fig 4A). These data thus demonstrate that a large subset of IMP2-controlled mRNAs bind to IMP2 directly, and that the rest are likely to be regulated secondarily, for example by IMP2-dependent TFs such as C/EBPβ/δ.

Analysis of *Cebpd* mRNA revealed consensus IMP2 binding sites within the 3' UTR that corresponded to high-confidence m^6A sites as predicted by the RMBase and SRAMP databases (Fig 4C, fig S8a, c). To better understand interactions between IMP2 and the *Cebpd* 3' UTR, we linked this sequence to a luciferase reporter with some or all of the predicted m^6A sites mutated to T (Fig 4C). These constructs were co-expressed with FLAG-tagged IMP2 in HEK293 cells, subjected to RIP with anti-FLAG Abs, and *Luciferase* mRNA enrichment was assessed by qPCR. There was substantial association of IMP2 with a *Luc* construct fused to the *Cebpd* 3' UTR sequence (Fig 4C). In contrast, a *Luc-Cebpd* 3' UTR construct in which all putative m^6A sites were mutated led to reduced enrichment of *Luciferase* mRNA upon IMP2-RIP. Mutation of just the two highest confidence m^6A sites (940, 977) similarly abolished IMP2 binding, demonstrating that these A sites are necessary for IMP2 binding. Interestingly, they are not sufficient, as a construct in which the remaining five putative m^6A sites were mutated also exhibited reduced IMP2 binding (Fig 4C). These results indicate that m^6A sites in the *Cebpd* 3'UTR mediate IMP2 occupancy. This finding is not only in agreement with published work on other m^6A-modified 3' UTRs, but is, to

our knowledge, the most detailed mutagenesis of a 3'UTR with respect to m^{6}A usage to date (59-61).

To confirm that IMP2 is a bona fide reader of m^{6}A-modified *Cebpd* mRNA, we employed an *in vitro* RNA pulldown assay using synthetic biotinylated 'bait' transcripts spanning the *Cebpd* 3'UTR that either m^{6}A-modified or unmodified (Fig 4D). These mRNAs were incubated with FLAG-tagged IMP2 derived from HEK293T cell overexpression. Samples were precipitated streptavidin-conjugated beads and immunoblotted with anti-FLAG. IMP2 interacted significantly more efficiently with the methylated bait than with the unmethylated controls, although at the highest concentrations IMP2 bound even to a non-modified transcript (Fig 4D). Therefore, m^{6}A modification within the 3' UTR markedly facilitates the binding of IMP2 to its client *Cebpd*.

RNA stability is a major mechanism by which inflammatory genes are regulated, so we evaluated the impact of IMP2 on C/EBP mRNA half-life using an mRNA decay assay (17, 62). *Imp2*$^{+/+}$ and *Imp2*$^{-/-}$ MEFs cells were primed with TNFα for 3 h, washed, treated with actinomycin D to stop new transcription, stimulated with IL-17, and mRNA measured over 90 minutes. Transcript half-life ($t_{½}$) was extrapolated by linear regression, as described (17, 63). IL-17 stabilized the *Cebpd* transcript in *Imp2*$^{+/+}$ cells, increasing its estimated $t_{½}$ from 86 to 117 minutes (Fig 4E). *Cebpd* mRNA decayed significantly more rapidly in *Imp2*$^{-/-}$ than in *Imp2*$^{+/+}$ cells. Unlike *Cebpd*, the stability of *Cebpb* mRNA was unaffected by *Imp2* deficiency or IL-17 treatment (Fig 4E).

IMP2 also regulates protein translation for some client transcripts (64, 65), so we evaluated occupancy of *Cebpd* and *Cebpb* mRNAs within the translation initiation complex by performing RIP of eIF4G (17, 66), a scaffolding subunit associated with mRNAs undergoing active translation. In control *Imp2*$^{+/+}$ cells, *Cebpd* and *Cebpb* but not *Gapdh* were enriched in eIF4G RIP preparations following IL-17 treatment. However, levels of *Cebpd* and *Cebpb* within the eIF4G complex were substantially reduced in *Imp2*$^{-/-}$ cells (Fig 4F), consistent with reduced C/EBPδ and C/EBPβ translational efficiency. Accordingly, *Cebpd* and *Cebpb* are subject to m^{6}A modification, which underlies the capacity of IMP2 to enhance C/EBPδ mRNA half-life and C/EBPδ and C/EBPβ protein expression.

HuR (*Elavl1)* and Act1 were previously shown to form dimeric complexes that mediate stability and translation of unstable mRNAs in the IL-17 pathway (24, 25). By co-IP, IMP2 associated constitutively and robustly with HuR but not with Act1 (Fig 5A). Like IMP2, knockdown of HuR impaired expression of *Cebpd, Il6* and *Lcn2* but not *Cebpb* (Fig 5B). Moreover, HuR deficiency was associated with reduced C/EBPδ and C/EBPβ protein expression (Fig 5C, D), in keeping with prior reports (67-70). These data suggest that IMP2 forms a complex with HuR to regulate C/EBPδ and C/EBPβ and consequently their downstream target genes.

IMP2 deficient mice resist IL-17-driven autoantibody-induced glomerulonephritis (AGN)

Accumulating reports implicate Th17 cells in autoantibody-mediated glomerulonephritis (AGN) (44, 71-76). Here we use an autologous model of rapidly progressive proliferative AGN in which disease is induced by administering rabbit anti-mouse glomerular basement

membrane (GBM) serum, leading to deposition of autoantibody complexes in glomeruli (72, 77, 78). The resulting renal pathology is IL-17-driven and shares clinical and pathological features of human crescentic GN (40, 71, 79). Lcn2 is a biomarker and driver of renal damage (80-84). Since *Lcn2* is regulated by IMP2, IL-17 and C/EBPs, we postulated that *Imp2*$^{-/-}$ mice would be resistant to AGN. *Imp2*$^{+/+}$ mice but not control *Act1*$^{-/-}$ mice developed elevated serum blood urea-nitrogen (BUN) and creatinine as well as marked histological renal pathology (Fig 6A) (72). *Imp2*$^{-/-}$ mice showed reduced BUN and creatinine levels (Fig 6A), reduced numbers of abnormal glomeruli, as well as decreased glomerular sclerosis, hypercellularity, and crescent formation (Fig 6B). Consistent with this, *Imp2*$^{-/-}$ mice had fewer kidney-infiltrating inflammatory monocytes compared to *Imp2*$^{+/+}$ littermates, and a trend to reduced neutrophils (Fig 6C, fig S9). Markers of nephropathy including *Lcn2, Il6* and *Kim1* (aka, Tim-1 (84)), were also elevated in *Imp2*$^{+/+}$ but not *Imp2*$^{-/-}$ or *Act1*$^{-/-}$ kidneys (Fig 6D).

To identify the cellular compartment where IMP2 functions during AGN, *Imp2*$^{+/+}$ or *Imp2*$^{-/-}$ mice were irradiated and adoptively transferred with autologous or reciprocal bone marrow (BM). After 6 weeks of engraftment, chimeric mice were subjected to AGN. *Imp2*$^{+/+}$ mice receiving *Imp2*$^{+/+}$ or *Imp2*$^{-/-}$ BM exhibited kidney dysfunction as indicated by elevated serum BUN and creatinine, whereas *Imp2*$^{-/-}$ mice receiving *Imp2*$^{+/+}$ or *Imp2*$^{-/-}$ BM showed kidney impairment (Fig 6E). Therefore, IMP2 acts in non-hematopoietic cells in AGN (85).

We next determined whether C/EBPs were regulated in the context of AGN and if so, whether this was IMP2-dependent. Indeed, *Cebpd* mRNA was elevated in total kidney tissue in *Imp2*$^{+/+}$ mice during AGN but not *Imp2*$^{-/-}$ littermates or *Act1*$^{-/-}$ mice (Fig. 7A). The major IL-17/TNFα-responsive cells implicated in AGN are renal tubular epithelial cells (RTECs) (71, 72). Intracellular staining of C/EBPδ in kidney homogenates showed that C/EBPδ was expressed in CD45^{-}CD133^{+} RTECs during AGN. Moreover, C/EBPδ staining was decreased in *Imp2*$^{-/-}$ compared to *Imp2*$^{+/+}$ RTECs (Fig 7B; fig S10a). Immunofluorescent staining of *Imp2*$^{+/+}$ control kidney sections revealed that C/EBPδ was high in glomeruli and low in RTECs in untreated mice, consistent with prior observations (86). During AGN, C/EBPδ was elevated in both medullary and cortical RTECs in *Imp2*$^{+/+}$ but not *Imp2*$^{-/-}$ mice (Fig 7C; enlarged images: fig S10b), in line with findings in another model of renal injury (87). C/EBPβ expression patterns were strikingly different from C/EBPδ, with far less prominent staining in glomeruli (Fig 7D). *Imp2*$^{-/-}$ mice exhibited reduced expression of C/EBPβ compared to *Imp2*$^{+/+}$ mice, especially in the cortex, regardless of AGN status (Fig 7D, enlarged images: fig S10c). Thus, IMP2 regulates C/EBPδ and C/EBPβ in kidney during AGN.

Many of the effects of IMP2 were evident not just after cytokine treatment but also to some extent at baseline (fig S5d). To rule out the possibility that the disease-promoting activity of IMP2 on AGN was due to baseline or developmental effects, we verified that there were no differences in the major immune compartments in *Imp2*$^{-/-}$ mice spleen or thymus (fig S11). *Imp2*$^{fl/fl}$ mice (88) were crossed to animals with a constitutive tamoxifen (TAM)-inducible Cre (*Rosa26*^{CreERT}), which permits gene deletion after administration of TAM. Mice were given TAM starting 1 day after induction of AGN and for the next 5 days

(Fig 8A). Deletion of *Imp2* was verified by qPCR of kidney (Fig 8B). Mice in which *Imp2* was deleted after AGN induction showed a similar improvement of kidney dysfunction as a complete knockout (Fig 8C). These data indicate that IMP2 effects on inflammation are not developmental and that blockade of IMP2 could potentially be targeted to ameliorate AGN.

DISCUSSION

It has long been appreciated that blocking cytokines such as TNFα is an effective treatment for many, though not all, autoimmune conditions. The contribution of the Th17/IL-17 pathway to autoimmunity has become appreciated with the success of biologic drugs targeting IL-17, the IL-17 receptor, or upstream regulators of Th17 cells (89-91). However, the cost of antibody-based drugs is often prohibitive, so there is an unmet need for therapies that are more universally applicable (4). In principle, any molecule in cytokine signal transduction could serve as a pharmacological target, but since our understanding of cytokine signaling is incomplete, there are hurdles to rational drug design (5).

Specificity in the RNA methylation pathway is particularly driven by m^6A readers (29), and in this regard IMP-family proteins were only recently recognized to be classified as such (35, 36). Moreover, IMP proteins have not been linked to autoimmunity or cytokine signal transduction (48), but rather to metabolism, stem cell maintenance, type 2 diabetes and cancer (37, 64, 85). Although one report described an *IGF2BP2* polymorphism in a psoriasis cohort, a condition that is strongly IL-17- and TNFα-driven, expression of *IGF2BP2* was linked only to altered triglycerides, not to psoriasis per se (92).

Glomerulonephritis (GN) causes mortality and morbidity in Goodpasture disease and ANCA vasculitis among other conditions (93). In mice, IL-17A, IL-17F and TNFα drive AGN pathology, and anti-IL-17 and anti-TNF blocking antibodies ameliorate disease in mouse models of crescentic GN (39, 44, 71-75, 94-97). Tissue-resident Th17 cells are implicated in human GN, and a recent report shows that these T cells recognize commensal microbes, such as *Staphylococcus aureus* and *Candida albicans* (39, 44, 94, 98, 99). In renal epithelial cells, IL-17 and TNFα signal cooperatively to activate inflammatory genes (7, 45, 71, 100, 101). Hence dual blockade of these cytokines is under consideration for treating autoimmunity (102). Autoimmunity is potentiated by multifactorial interacting gene networks, and decades of research in both humans and animal models of disease has underscored this complexity. Several genes controlled by IMP2 help explain its contribution to cytokine-mediated AGN, particularly *Lcn2* and *Il6* (81, 82, 103). Though IMP2 regulates lamininβ2 (*Lamb2*), a glomerular basement membrane component that promotes renal barrier permeability, *Lamb2* is not regulated by IL-17 in murine AGN (104). In a model of anti-Thy1-induced GN, loss of C/EBPδ protected from disease, though its connections to IL-17 were unknown at the time that study was conducted (86). Conversely, C/EBPδ-deficiency caused worse pathology in the unilateral ureteral obstruction (UUO) model of kidney fibrosis (87). Strikingly, IL-17 signaling similarly attenuates pathology in UUO (105) and RTECs are the dominant cell type expressing C/EBPδ and responding to IL-17 in the kidney (87)(106, 107).

We originally linked C/EBPβ and C/EBPδ to IL-17 signaling in 2004, finding that C/EBPδ in particular contributes to IL-17 activation of downstream genes and to signaling cooperativity between IL-17 and TNFα (7). The role of C/EBPβ in the IL-17 pathway is not always straightforward, as it serves as a transcriptional activator (7, 8, 108) but can also be a repressor, for example when subject to phosphorylation (19, 109). The present work led to the unexpected observation that C/EBPβ and C/EBPδ expression is controlled at a post-transcriptional level by the noncanonical m^6A reader IMP2. Genes regulated by C/EBPs (e.g., *Il6, Lcn2*) are consequently IMP2-dependent. Interestingly, IMP2 was the only m^6A reader seen to increase cytokine-induced mRNAs in these studies, whereas the more common YTH-domain readers did not, thus revealing considerable specificity in terms of how the m^6A pathway operates in response to cytokines. Here we confirm that TNFα does not upregulate C/EBPδ (46), representing a divergence in the mechanisms by which inflammatory cytokines trigger downstream gene expression. Thus, the m^6A/IMP2/C/EBP axis represents a previously-unrecognized avenue of signal activation that is likely to apply to many cytokines, probably in distinct and specific modalities.

In recent years, IL-17 has become appreciated as a potent regulator of post-transcriptional gene expression (5, 110-112). Moreover, post-transcriptional regulation pathways activated by IL-17 exhibit crosstalk with transcriptional signaling in intricate ways. For example, IκBξ, a noncanonical member of the NF-κB family, is required for many IL-17-induced genes (113). The mRNA encoding IκBξ (*Nfkbiz*) is intrinsically unstable, subject to both positive and negative regulation by IL-17-activated RBPs. For example, the endoribonuclease Regnase-1 (MCPIP1) degrades *Nfkbiz* upon binding the 3' UTR (26). Regnase-1 mRNA (*Zc3h12a*) is subject to autoregulation as well as control by the DDX3X RNA helicase (27, 114). Additionally, Regnase-1 activity is counteracted by Arid5a, which binds to *Nfkbiz* and thereby enhances translation of IκBξ (17), which in turn triggers a cascade of downstream IL-17-dependent genes. Arid5a controls translation of C/EBPβ, but surprisingly does not impact C/EBPδ (17). In contrast, IMP2 did not impact *Nfkbiz* or *Zc3h12a* expression. Although IL-17 leads to inducible phosphorylation of C/EBPβ by ERK and GSK3β (19, 20), IMP2 did not impact IL-17-dependent activation of MAPK pathways (fig S12). In these studies, only a subset of IL-17-dependent transcripts are regulated by IMP2. Collectively, these data suggest that IMP2 operates in a distinct and specific post-transcriptional pathway (Fig. 8D).

HuR is an RBP that influences many facets of mRNA fate, including transcript stability and translation. Upon IL-17 signaling, HuR binds to Act1, a multifunctional signaling protein required for all known IL-17-dependent signals. Act1, in conjunction with TRAF2, has the capacity to bind to target mRNAs and control their stability as well as direct translation (24, 25). Here we show that IMP2 interacts with HuR but not with Act1, in agreement with findings that HuR facilitates IMP2 function (35). HuR has been shown to regulate C/EBPβ and C/EBPδ mRNA nuclear export, translation, and stability (67-70). Hence, there is remarkable complexity, specificity and crosstalk among the transcriptional and post-transcriptional regulators that determine the output of cytokine-derived signals (5).

The concept that IMP2 may exert distinct effects depending on its client mRNA has precedent (54, 88, 115, 116), but the basis of its binding selectivity was elusive until the

discovery that IMP2 recognizes N^6-methyladenosine (m^6A) (35). This RNA modification is mediated by core methyltransferases (e.g., METTL3/14) and is regulated dynamically by demethylase enzymes (e.g., FTO). Although there are only limited studies interrogating the functional significance m^6A in the immune system, this modification occurs in innate immunity in response to viral infection (32, 33), and loss of METTL3 in T cells was reported to impair T cell homeostasis through SOCS-mediated inhibition of IL-7/STAT5 signaling (30). METTL3 in T cells also controlled IL-2/STAT5 and thus Treg function (31). By evaluating the upstream methylase METTL3, those studies implicated m^6A broadly in immune system control, but as yet the specific readers recognizing the m^6A RNA mark have not been described in these settings.

The establishment of a rapid inflammatory response through activation of post-transcriptional events requires a tonic level of mRNA expression (112). IMP2 has potent effects on RNAs induced by cytokines, but also influences their baseline expression (54, 58, 115). In agreement with this, in the absence of a stressor, the immune system appeared normal in *Imp2*$^{-/-}$ mice. Moreover, IMP2-dependent effects on AGN were not caused by aberrant developmental issues, since deletion of IMP2 after AGN onset resulted in a similar suppression of renal damage as a full IMP2 knockout. Therefore, IMP2 is not merely a rheostat that alters the ability of cells to respond to all signals, but rather exerts selective effects, many of which rely on the C/EBP pathway.

In summary, these findings uncover a new role for m^6A epitranscriptomic RNA marks and the noncanonical m^6A reader IMP2 in cytokine-driven autoimmunity. The capacity of IMP2 to direct posttranscriptional regulation of *Cebpd* and *Cebpb* potentiates expression of genes reliant on these TFs, which in turn underlie pathology in autoimmune inflammation of the kidney (Fig 8D). Exploiting RNA therapeutically is attractive given its potential for exquisite specificity and the possibility of targeting otherwise “un-druggable” molecules. Accordingly, strategies are in development that target RNA or RBPs (117, 118). In the IL-17 pathway, a preclinical study using aptamers to target the RNA-binding properties of Act1 elegantly illustrated proof-of-principle for this concept (24). Still, taking full advantage of RNA requires a complete understanding of the molecular players involved, especially RBPs, and the relevant client transcript mRNAs regulated within pertinent target cells.

Materials and Methods

Study design

The objective of this study was to determine how C/EBPs are regulated in the IL-17 signal pathway. We used cell culture studies and a model of AGN to define the role of m^6A pathway components on IL-17 signaling. Sample sizes were determined by power analyses from pilot or previously published data. Mice of both sexes were assigned randomly to experimental cohorts. Unless noted, experiments were done 3 or more independent times. Data from multiple experiments were pooled unless noted. Investigators were not blinded to groups except for immunofluorescent image analysis. No data were excluded. Endpoints were selected based on prior studies. The details of the reagents used are provided in Table S2.

Mice

All mice were on the C57BL/6 background. Cohorts were age- and sex-matched. *Act1*$^{-/-}$ mice were from NIH and *Imp2*$^{-/-}$ mice were obtained under MTA from Oxford, UK. Wild type (WT) controls were usually derived from breeding of heterozygote mice to generate littermate controls. In some instances, WT mice were from Taconic Farms or The Jackson Laboratory, and were co-housed with experimental cohorts for at least 3 weeks to normalize microbiota. Mice were housed in SPF conditions. Protocols were approved by the University of Pittsburgh IACUC.

AGN

AGN was induced by i.p. injection of rabbit IgG (0.1 mg/ml) in CFA (2.5 mg/ml; Sigma, St. Louis, MO) on day -3. Heat-inactivated rabbit anti-mouse GBM serum (Lampire Biological Laboratories, Pipersville, PA) was injected (100 μl) i.v. (71). BUN and creatinine levels were measured on days 7 or 14 by a BUN ELISA kit (Bioo Scientific, Austin, TX) or a QuantiChrom Creatinine Assay Kit (BioAssay Systems, DICT-500). Kidney sections were stained with H&E and images acquired on an EVOS FL Auto Imaging System.

Radiation Chimeras

On day −1, recipients (WT, CD45.1) or *Imp2*$^{-/-}$ (CD45.2) were given sulfamethoxazole and trimethoprim in drinking water for 10 days. On day 0, mice were irradiated (900 rad). On day 1, 5 ×10^6 donor femoral BM cells were injected i.v. into recipients. After 6 weeks, BM reconstitution was verified by flow cytometry.

Cell Culture

MEFs, HK-2 and HEK293T cells were cultured in α-minimum essential medium (α-MEM; Sigma-Aldrich, St. Louis MO) with L-glutamine, antibiotics and 10–15% FBS. HK-2 cells (ATCC) were cultured in DMEM/F12 (Gibco), antibiotics and 10% FBS. IL-17, IL-17F and TNFα (PeproTech, Rocky Hill, NJ) were used at 200 and 10 ng/ml. Actinomycin D (Sigma-Aldrich) was used at 10 μg/ml.

siRNA, Plasmids and Luciferase assays

ON-TARGETplus SMARTpool siRNAs were from Dharmacon (Lafayette, CO). MEFs and HK-2 cells were seeded overnight in antibiotic-free media and transfected 18 h later with 50 nM siRNA in DharmaFECT Reagent 1. Culture media was replaced after 24 h, and cytokines administered 24 h later. The *Lcn2* and *Il6* promoter constructs were described (6, 51). MEFs were transfected with FuGENE HD (Promega). HEK293T cells were transfected using $CaPO_4$. Constructs containing the 5'UTR, coding sequences and 3'UTR of murine *Cebpb* was synthesized by Bon Opus Biosciences (Millburn, NJ). Luciferase assays were performed with the Dual-Luciferase Reporter Assay System (Promega) and normalized to a *Renilla* luciferase control (17).

qPCR, RNA-Seq, RIP-Seq

RNA was isolated with RNeasy Mini Kits (Qiagen), and cDNA was synthesized by SuperScript III First Strand Kits (Thermo Fisher Scientific, Waltham MA). Real-time qPCR

was performed with SYBR Green FastMix ROX (Quanta Biosciences) on a 7300 Real-Time instrument (Applied Biosystems), normalized to *Gapdh*. Primers were from QuantiTect Primer Assays (QIAGEN). RNASeq libraries were prepared from MEF mRNA (Nextera XT Kit). RNASeq was performed on Illumina NextSeq 500 by the Health Sciences Sequencing Core at the University of Pittsburgh.

For RIP-Seq, libraries were generated using SMART-Seq v4 Ultra Low Input RNA kit (Takara Biosciences) and sequenced on a NextSeq500. Raw reads were aligned to mm10 using STAR (119) followed by identification of global binding of IMP2 using Piranha (55). Differentially enriched IMP2 interactions were identified with DESeq2 (56) by comparing 3 replicates of IMP2-RIP-seq data and control IgG. Identification of IMP2 motifs (35, 120) was performed using MDS^2 (57) and viewed using Integrative Genomics Viewer (Broad Institute).

Immunoblotting, Immunoprecipitation

Western blotting and IPs were performed as described (17). Immunoblotting Abs: METTL3 (Proteintech, 1:1000), FTO (Santa Cruz Biotechnology, 1:1000), IMP2 (MBL, 1:1000; Cell Signaling, 1:1000), C/EBPδ (Cell Signaling, 1:1000; Santa Cruz Biotechnology, 1:1000), C/EBPβ (Biolegend, 1:500; Santa Cruz Biotechnology, 1:1000), YY1 (Santa Cruz Biotechnology, 1:1000), β-actin (Abcam, 1:25,000), phospho-p38 MAPK, p38 MAPK, phospho-JNK , JNK, phospho-p44/42, p44/42 (Cell Signaling, 1:1000), eIF4G (Cell Signaling, 1:1000). Blots viewed with a FluorChem E imager (Protein Simple, Santa Clara CA).

RNA immunoprecipitation (RIP) and *in vitro* RNA pulldown

For IMP2 RIPs, extracts were isolated with lysis buffer [100 mM KCl, 5 mM $MgCl_2$, 10 mM HEPES (pH 7.0), 0.5% NP-40, 1 mM dithiothreitol] with RNAseOUT (100 U/ml; Invitrogen). For eIF4G RIP, extracts were isolated with lysis buffer [0.3% CHAPS, 40 mM HEPES (pH 7.5), 120 mM NaCl, 1 mM EDTA, 10 mM sodium pyrophosphate, 10 mM β-glycerophosphate, 50 mM NaF, 1.5 mM sodium orthovanadate, 1 mM DTT]. Buffers included a protease inhibitor cocktail (Sigma-Aldrich). Lysates were precleared protein A agarose (Roche) or protein G–conjugated magnetic Dynabeads (ThermoFisher) and immunoprecipitated with Abs against IMP2 (MBL), eIF4G (Cell Signaling) or FLAG (Sigma). Beads were washed with NT2 buffer and digested with DNase I (Roche Applied Science) and protease K (Sigma). Total RNA was extracted with acid phenol or TRIzol.

For RNA pulldowns, biotinylated RNA corresponding to the *Cebpd* 3'UTR (bases 863-982) was synthesized with specified adenosines subject to m^6A modification (Dharmacon). RNAs were incubated with lysates from HEK293T cells transfected with FLAG-IMP2, precipitated with streptavidin Dynabeads M-280 (ThermoFisher), isolated by magnetic separation and subjected to immunoblotting.

For m^6A RIP (MeRIP) (32), 20–50 μg RNA was fragmented and purified by ethanol precipitation. 0.1 fmol of a control m^6A-modified *Gaussia* luciferase RNA or unmodified *Cypridina* luciferase RNA (supplied with the EpiMark *N6*-methyladenosine Enrichment kit) were spiked in each sample. For RIP, Protein G Dynabeads (Thermo Fisher) were washed in

MeRIP buffer (150 mM NaCl, 10 mM Tris-HCl [pH 7.5], 0.1% NP-40), and incubated with anti-m^{6}A Abs for 2 h at 4°C. After washing, anti-m^{6}A conjugated beads were incubated with mRNA for 4 h in RNasin (Promega). Up to 3% of mRNA was used for input. Beads were washed with MeRIP buffer, low salt wash buffer (50 mM NaCl, 10 mM Tris-HCl [pH 7.5], 0.1% NP-40), and wash buffer (500 mM NaCl, 10 mM Tris-HCl [pH 7.5], 0.1% NP-40). m^{6}A-modified RNA was eluted in MeRIP buffer containing 5 mM m^{6}A salt (Santa Cruz Biotechnology). Eluates were pooled and concentrated by ethanol precipitation. Input and IP fractions were reverse transcribed using the iScript cDNA synthesis kit (BioRad) and subjected to qPCR.

Immunofluorescence, flow cytometry

Frozen sections (8 μm) were fixed in 100% methanol and blocked with 5% goat serum (500622, Life Technologies) in Triton X. Primary antibodies were incubated overnight: C/EBPδ (Abcam, 1:200), normal rabbit IgG (Abcam, 1:200), C/EBPβ (Abcam, 1:200) and rabbit monoclonal IgG (Abcam, 1:200). Slides were incubated with goat anti-Rabbit Cy3 antibody (A15020, Thermo Fisher) or DAPI. Slides were visualized on an EVOS FL microscope (Life Technologies).

For flow cytometry, kidneys were harvested following perfusion with PBS. Cells were digested with collagenase IV (1mg/mL) in HBSS. Antibodies: anti-CD45 (clone 30-F11, Thermo Fisher), anti-Ly6G (clone 1A8, BD Biosciences), anti-Ly6C (clone HK1.4, eBioscience), anti-CD11b (clone M1/70, BioLegend), anti-CD133 (clone 13A4, Thermo Fisher), anti-C/EBPδ (Abcam, 1:500), rabbit polyclonal Abs (Abcam, 1:500), and secondary goat anti-Rabbit Alexa Fluor 488 Abs (Thermo Fisher). Dead cells were excluded using Ghost Dye (eBioscience). C/EBPδ intracellular staining was performed with the FOXP3 staining kit (eBioscience). Data acquired with LSR Fortessa and analyzed using FlowJo software (TreeStar).

RNA decay assays

MEFs were primed with TNFα (10 ng/ml) for 3 h and treated with 10 μg/ml actinomycin D (ActD; Sigma-Aldrich) ± 200 ng/ml IL-17 as described (17). For each mRNA, quantity (%) was calculated by normalizing ΔΔCt to the ΔΔCt of samples primed with TNFα.

Statistics

One-way ANOVA with post hoc Tukey's analysis or Student's *t*-test was used to assess significance, $P < 0.05$ considered significant. Data were analyzed on GraphPad Prism. Each symbol represents one mouse.

Supplementary Material

Refer to Web version on PubMed Central for supplementary material.

Acknowledgments:

We thank the HSSC@CHP for RNAseq support. We thank L. Minichiello, University of Oxford, and J. Avruch, Harvard, for *Imp2*$^{-/-}$ mice and valuable suggestions. S. Majumder and MJ McGeachy provided helpful input. We are grateful to Ulrich Siebenlist (deceased) for *Act1*$^{-/-}$ mice.

Funding:

NIH supported SLG (DE022550, AI107825, AI147383), PSB (DK104680, AI142354) and SMH (AI125416). SLG and PSB were supported by the Rheumatology Research Foundation. SMH was supported by the Burroughs Wellcome Fund. Work was also supported in part by the University of Pittsburgh Center for Research Computing.

References and Notes

1. Helmick CGet al., Estimates of the prevalence of arthritis and other rheumatic conditions in the United States. Part I. Arthritis Rheum58, 15–25 (2008). [PubMed: 18163481]
2. A. C. o. Rheumatology. (American College of Rheumatology, 2012).
3. McGeachy MJ, Cua DJ, Gaffen SL, The IL-17 Family of Cytokines in Health and Disease. Immunity50, 892–906 (2019). [PubMed: 30995505]
4. Slivka PFet al., Small Molecule and Pooled CRISPR Screens Investigating IL17 Signaling Identify BRD2 as a Novel Contributor to Keratinocyte Inflammatory Responses. ACS Chem Biol14, 857–872 (2019). [PubMed: 30938974]
5. Li X, Bechara R, Zhao J, McGeachy MJ, Gaffen SL, Interleukin 17 receptor-based signaling and implications for disease. Nature Immunology20, 1594–1602 (2019). [PubMed: 31745337]
6. Shen F, Hu Z, Goswami J, Gaffen SL, Identification of common transcriptional regulatory elements in interleukin-17 target genes. J Biol Chem281, 24138–24148 (2006). [PubMed: 16798734]
7. Ruddy MJet al., Functional cooperation between interleukin-17 and tumor necrosis factor-a is mediated by CCAAT/enhancer binding protein family members. J Biol Chem279, 2559–2567 (2004). [PubMed: 14600152]
8. Patel DNet al., Interleukin-17 stimulates C-reactive protein expression in hepatocytes and smooth muscle cells via p38 MAPK and ERK1/2-dependent NF-kappaB and C/EBPbeta activation. J Biol Chem282, 27229–27238 (2007). [PubMed: 17652082]
9. Karlsen JR, Borregaard N, Cowland JB, Induction of neutrophil gelatinase-associated lipocalin expression by co-stimulation with interleukin-17 and tumor necrosis factor-alpha is controlled by IkappaB-zeta but neither by C/EBP-beta nor C/EBP-delta. J Biol Chem285, 14088–14100 (2010). [PubMed: 20220144]
10. Slowikowski Ket al., CUX1 and IkappaBzeta (NFKBIZ) mediate the synergistic inflammatory response to TNF and IL-17A in stromal fibroblasts. Proc Natl Acad Sci U S A117, 5532–5541 (2020). [PubMed: 32079724]
11. Qian Yet al., The adaptor Act1 is required for interleukin 17-dependent signaling associated with autoimmune and inflammatory disease. Nat Immunol8, 247–256 (2007). [PubMed: 17277779]
12. Chang SH, Park H, Dong C, Act1 adaptor protein is an immediate and essential signaling component of interleukin-17 receptor. J Biol Chem281, 35603–35607 (2006). [PubMed: 17035243]
13. Amatya N, Garg AV, Gaffen SL, IL-17 Signaling: The Yin and the Yang. Trends Immunol38, 310–322 (2017). [PubMed: 28254169]
14. Tsukada J, Yoshida Y, Kominato Y, Auron PE, The CCAAT/enhancer (C/EBP) family of basic-leucine zipper (bZIP) transcription factors is a multifaceted highly-regulated system for gene regulation. Cytokine54, 6–19 (2011). [PubMed: 21257317]
15. Ko CY, Chang WC, Wang JM, Biological roles of CCAAT/Enhancer-binding protein delta during inflammation. J Biomed Sci22, 6 (2015). [PubMed: 25591788]
16. Ramji DP, Foka P, CCAAT/enhancer-binding proteins: structure, function and regulation. Biochem J365, 561–575. (2002). [PubMed: 12006103]
17. Amatya Net al., IL-17 integrates multiple self-reinforcing, feed-forward mechanisms through the RNA-binding protein Arid5a. Science Signaling11, eaat4617 (2018). [PubMed: 30301788]

18. Shen F, Gaffen SL, Structure-function relationships in the IL-17 receptor: Implications for signal transduction and therapy. Cytokine41, 92–104 (2008). [PubMed: 18178098]
19. Shen Fet al., IL-17 Receptor Signaling Inhibits C/EBPbeta by Sequential Phosphorylation of the Regulatory 2 Domain. Sci Signal2, ra8 (2009). [PubMed: 19244213]
20. Tang QQet al., Sequential phosphorylation of CCAAT enhancer-binding protein beta by MAPK and glycogen synthase kinase 3beta is required for adipogenesis. Proc Natl Acad Sci U S A102, 9766–9771 (2005). [PubMed: 15985551]
21. Pulido-Salgado M, Vidal-Taboada JM, Saura J, C/EBPbeta and C/EBPdelta transcription factors: Basic biology and roles in the CNS. Prog Neurobiol132, 1–33 (2015). [PubMed: 26143335]
22. Huber R, Pietsch D, Panterodt T, Brand K, Regulation of C/EBPbeta and resulting functions in cells of the monocytic lineage. Cell Signal24, 1287–1296 (2012). [PubMed: 22374303]
23. Shi JH, Sun SC, Tumor Necrosis Factor Receptor-Associated Factor Regulation of Nuclear Factor kappaB and Mitogen-Activated Protein Kinase Pathways. Front Immunol9, 1849 (2018). [PubMed: 30140268]
24. Herjan Tet al., IL-17-receptor-associated adaptor Act1 directly stabilizes mRNAs to mediate IL-17 inflammatory signaling. Nat Immunol19, 354–365 (2018). [PubMed: 29563620]
25. Herjan Tet al., HuR is required for IL-17-induced Act1-mediated CXCL1 and CXCL5 mRNA stabilization. J Immunol191, 640–649 (2013). [PubMed: 23772036]
26. Garg AVet al., MCPIP1 Endoribonuclease Activity Negatively Regulates Interleukin-17-Mediated Signaling and Inflammation. Immunity43, 475–487 (2015). [PubMed: 26320658]
27. Somma Det al., CIKS/DDX3X Interaction Controls the Stability of the Zc3h12a mRNA Induced by IL-17. J Immunol194, 3286–3294 (2015). [PubMed: 25710910]
28. Shi H, Wei J, He C, Where, When, and How: Context-Dependent Functions of RNA Methylation Writers, Readers, and Erasers. Mol Cell74, 640–650 (2019). [PubMed: 31100245]
29. Zaccara S, Ries RJ, Jaffrey SR, Reading, writing and erasing mRNA methylation. Nat Rev Mol Cell Biol20, 608–624 (2019). [PubMed: 31520073]
30. Li HBet al., m(6)A mRNA methylation controls T cell homeostasis by targeting the IL-7/STAT5/SOCS pathways. Nature548, 338–342 (2017). [PubMed: 28792938]
31. Tong Jet al., m(6)A mRNA methylation sustains Treg suppressive functions. Cell Res28, 253–256 (2018). [PubMed: 29303144]
32. Gokhale NSet al., Altered m(6)A Modification of Specific Cellular Transcripts Affects Flaviviridae Infection. Mol Cell, (2019).
33. Liu Yet al., N (6)-methyladenosine RNA modification-mediated cellular metabolism rewiring inhibits viral replication. Science365, 1171–1176 (2019). [PubMed: 31439758]
34. Paramasivam A, Vijayashree Priyadharsini J, Novel insights into m6A modification in circular RNA and implications for immunity. Cell Mol Immunol, (2020).
35. Huang Het al., Recognition of RNA N(6)-methyladenosine by IGF2BP proteins enhances mRNA stability and translation. Nat Cell Biol20, 285–295 (2018). [PubMed: 29476152]
36. Huang H, Weng H, Chen J, m(6)A Modification in Coding and Non-coding RNAs: Roles and Therapeutic Implications in Cancer. Cancer Cell37, 270–288 (2020). [PubMed: 32183948]
37. Shulman Z, Stern-Ginossar N, The RNA modification N(6)-methyladenosine as a novel regulator of the immune system. Nat Immunol21, 501–512 (2020). [PubMed: 32284591]
38. McAdoo SP, Pusey CD, Anti-Glomerular Basement Membrane Disease. Clin J Am Soc Nephrol12, 1162–1172 (2017). [PubMed: 28515156]
39. Biswas P, IL-17 in renal immunity and autoimmunity. J Immunol201, 3153–3159 (2018). [PubMed: 30455371]
40. Kurts C, Panzer U, Anders HJ, Rees AJ, The immune system and kidney disease: basic concepts and clinical implications. Nat Rev Immunol13, 738–753 (2013). [PubMed: 24037418]
41. Lahmer T, Heemann U, Anti-glomerular basement membrane antibody disease: a rare autoimmune disorder affecting the kidney and the lung. Autoimmun Rev12, 169–173 (2012). [PubMed: 22546293]
42. Ernandez T, Mayadas TN, The Changing Landscape of Renal Inflammation. Trends Mol Med22, 151–163 (2016). [PubMed: 26778189]

43. Shlomchik MJ, Activating systemic autoimmunity: B's, T's, and tolls. Curr Opin Immunol21, 626–633 (2009). [PubMed: 19800208]
44. Krebs CFet al., Pathogen-induced tissue-resident memory TH17 (TRM17) cells amplify autoimmune kidney disease. Sci Immunol5, (2020).
45. Shen F, Ruddy MJ, Plamondon P, Gaffen SL, Cytokines link osteoblasts and inflammation: microarray analysis of interleukin-17- and TNF-alpha-induced genes in bone cells. J Leukoc Biol77, 388–399 (2005). [PubMed: 15591425]
46. Sonder SUet al., IL-17-induced NF-kappaB activation via CIKS/Act1: physiologic significance and signaling mechanisms. J Biol Chem286, 12881–12890 (2011). [PubMed: 21335551]
47. Johansen Cet al., IkappaBzeta is a key driver in the development of psoriasis. Proc Natl Acad Sci U S A112, E5825–5833 (2015). [PubMed: 26460049]
48. Dai N, The Diverse Functions of IMP2/IGF2BP2 in Metabolism. Trends Endocrinol Metab31, 670–679 (2020). [PubMed: 32586768]
49. Ryan MJet al., HK-2: an immortalized proximal tubule epithelial cell line from normal adult human kidney. Kidney Int45, 48–57 (1994). [PubMed: 8127021]
50. Litvak Vet al., Function of C/EBPdelta in a regulatory circuit that discriminates between transient and persistent TLR4-induced signals. Nat Immunol10, 437–443 (2009). [PubMed: 19270711]
51. Eickelberg Oet al., Transforming growth factor-beta1 induces interleukin-6 expression via activating protein-1 consisting of JunD homodimers in primary human lung fibroblasts. J Biol Chem274, 12933–12938. (1999). [PubMed: 10212284]
52. Zhou Y, Zeng P, Li YH, Zhang Z, Cui Q, SRAMP: prediction of mammalian N6-methyladenosine (m6A) sites based on sequence-derived features. Nucleic Acids Res44, e91 (2016). [PubMed: 26896799]
53. Xuan JJet al., RMBase v2.0: deciphering the map of RNA modifications from epitranscriptome sequencing data. Nucleic Acids Res46, D327–D334 (2018). [PubMed: 29040692]
54. Hafner Met al., Transcriptome-wide identification of RNA-binding protein and microRNA target sites by PAR-CLIP. Cell141, 129–141 (2010). [PubMed: 20371350]
55. Uren PJet al., Site identification in high-throughput RNA-protein interaction data. Bioinformatics28, 3013–3020 (2012). [PubMed: 23024010]
56. Love MI, Huber W, Anders S, Moderated estimation of fold change and dispersion for RNA-seq data with DESeq2. Genome Biol15, 550 (2014). [PubMed: 25516281]
57. Gao T, Shu J, Cui J, A systematic approach to RNA-associated motif discovery. BMC Genomics19, 146 (2018). [PubMed: 29444662]
58. Dai Net al., IGF2BP2/IMP2-Deficient mice resist obesity through enhanced translation of Ucp1 mRNA and Other mRNAs encoding mitochondrial proteins. Cell Metab21, 609–621 (2015). [PubMed: 25863250]
59. McFadden MJet al., Post-transcriptional regulation of antiviral gene expression by N6-methyladenosine. Cell Rep34, 108798 (2021). [PubMed: 33657363]
60. Gokhale NSet al., Altered m(6)A Modification of Specific Cellular Transcripts Affects Flaviviridae Infection. Mol Cell77, 542–555 (2020). [PubMed: 31810760]
61. Regue Let al., RNA m6A reader IMP2/IGF2BP2 promotes pancreatic beta-cell proliferation and insulin secretion by enhancing PDX1 expression. Mol Metab, 101209 (2021). [PubMed: 33705986]
62. Henness Set al., IL-17A augments TNF-alpha-induced IL-6 expression in airway smooth muscle by enhancing mRNA stability. J Allergy Clin Immunol114, 958–964 (2004). [PubMed: 15480342]
63. Masuda Ket al., Arid5a controls IL-6 mRNA stability, which contributes to elevation of IL-6 level in vivo. Proc Natl Acad Sci U S A, (2013).
64. Christiansen J, Kolte AM, Hansen T, Nielsen FC, IGF2 mRNA-binding protein 2: biological function and putative role in type 2 diabetes. J Mol Endocrinol43, 187–195 (2009). [PubMed: 19429674]
65. Dai Net al., mTOR phosphorylates IMP2 to promote IGF2 mRNA translation by internal ribosomal entry. Genes Dev25, 1159–1172 (2011). [PubMed: 21576258]

66. Lahr RMet al., La-related protein 1 (LARP1) binds the mRNA cap, blocking eIF4F assembly on TOP mRNAs. Elife6, (2017).

67. Cherry J, Jones H, Karschner VA, Pekala PH, Post-transcriptional control of CCAAT/enhancer-binding protein beta (C/EBPbeta) expression: formation of a nuclear HuR-C/EBPbeta mRNA complex determines the amount of message reaching the cytosol. J Biol Chem283, 30812–30820 (2008). [PubMed: 18678862]

68. Gantt K, Cherry J, Tenney R, Karschner V, Pekala PH, An early event in adipogenesis, the nuclear selection of the CCAAT enhancer-binding protein {beta} (C/EBP{beta}) mRNA by HuR and its translocation to the cytosol. J Biol Chem280, 24768–24774 (2005). [PubMed: 15863502]

69. Hsiao YWet al., CCAAT/enhancer binding protein delta in macrophages contributes to immunosuppression and inhibits phagocytosis in nasopharyngeal carcinoma. Sci Signal6, ra59 (2013). [PubMed: 23861541]

70. Li B, Si J, DeWille JW, Ultraviolet radiation (UVR) activates p38 MAP kinase and induces post-transcriptional stabilization of the C/EBPdelta mRNA in G0 growth arrested mammary epithelial cells. J Cell Biochem103, 1657–1669 (2008). [PubMed: 17902160]

71. Ramani Ket al., An essential role of interleukin-17 receptor signaling in the development of autoimmune glomerulonephritis. J Leukoc Biol96, 463–472 (2014). [PubMed: 24935958]

72. Pisitkun Pet al., Interleukin-17 cytokines are critical in development of fatal lupus glomerulonephritis. Immunity37, 1104–1115 (2012). [PubMed: 23123062]

73. Krohn Set al., IL-17C/IL-17 Receptor E Signaling in CD4(+) T Cells Promotes TH17 Cell-Driven Glomerular Inflammation. J Am Soc Nephrol29, 1210–1222 (2018). [PubMed: 29483158]

74. Riedel JHet al., IL-17F Promotes Tissue Injury in Autoimmune Kidney Diseases. J Am Soc Nephrol27, 3666–3677 (2016). [PubMed: 27030744]

75. Turner JEet al., IL-17A production by renal gammadelta T cells promotes kidney injury in crescentic GN. J Am Soc Nephrol23, 1486–1495 (2012). [PubMed: 22797181]

76. Mohamed Ret al., Low-Dose IL-17 Therapy Prevents and Reverses Diabetic Nephropathy, Metabolic Syndrome, and Associated Organ Fibrosis. J Am Soc Nephrol27, 745–765 (2016). [PubMed: 26334030]

77. Du Y, Fu Y, Mohan C, Experimental anti-GBM nephritis as an analytical tool for studying spontaneous lupus nephritis. Arch Immunol Ther Exp (Warsz)56, 31–40 (2008). [PubMed: 18250969]

78. Fu Y, Du Y, Mohan C, Experimental anti-GBM disease as a tool for studying spontaneous lupus nephritis. Clin Immunol124, 109–118 (2007). [PubMed: 17640604]

79. Krebs CF, Schmidt T, Riedel JH, Panzer U, T helper type 17 cells in immune-mediated glomerular disease. Nat Rev Nephrol13, 647–659 (2017). [PubMed: 28781371]

80. Viau Aet al., Lipocalin 2 is essential for chronic kidney disease progression in mice and humans. J Clin Invest120, 4065–4076 (2010). [PubMed: 20921623]

81. Yang CCet al., Urinary neutrophil gelatinase-associated lipocalin is a potential biomarker for renal damage in patients with systemic lupus erythematosus. J Biomed Biotechnol2012, 759313 (2012). [PubMed: 22500106]

82. Torres-Salido MTet al., Neutrophil gelatinase-associated lipocalin as a biomarker for lupus nephritis. Nephrol Dial Transplant29, 1740–1749 (2014). [PubMed: 24711435]

83. Haase M, Haase-Fielitz A, Bellomo R, Mertens PR, Neutrophil gelatinase-associated lipocalin as a marker of acute renal disease. Curr Opin Hematol18, 11–18 (2011). [PubMed: 21102325]

84. Satirapoj B, Tubulointerstitial Biomarkers for Diabetic Nephropathy. J Diabetes Res2018, 2852398 (2018). [PubMed: 29577044]

85. Cao J, Mu Q, Huang H, The Roles of Insulin-Like Growth Factor 2 mRNA-Binding Protein 2 in Cancer and Cancer Stem Cells. Stem Cells Int2018, 4217259 (2018). [PubMed: 29736175]

86. Takeji Met al., CCAAT/Enhancer-binding protein delta contributes to myofibroblast transdifferentiation and renal disease progression. J Am Soc Nephrol15, 2383–2390 (2004). [PubMed: 15339987]

87. Duitman Jet al., CCAAT-enhancer binding protein delta (C/EBPdelta) attenuates tubular injury and tubulointerstitial fibrogenesis during chronic obstructive nephropathy. Lab Invest94, 89–97 (2014). [PubMed: 24247561]

88. Degrauwe Net al., The RNA Binding Protein IMP2 Preserves Glioblastoma Stem Cells by Preventing let-7 Target Gene Silencing. Cell Rep15, 1634–1647 (2016). [PubMed: 27184842]

89. Lubberts E, The IL-23-IL-17 axis in inflammatory arthritis. Nat Rev Rheumatol11, 415–429 (2015). [PubMed: 25907700]

90. Gaffen SL, Jain R, Garg A, Cua D, IL-23-IL-17 immune axis: From mechanisms to therapeutic testing. Nat Rev Immunol14, 585–600 (2014). [PubMed: 25145755]

91. Koenders MI, van den Berg WB, Novel therapeutic targets in rheumatoid arthritis. Trends Pharmacol Sci36, 189–195 (2015). [PubMed: 25732812]

92. Kargun Ket al., IGF2BP2 gene polymorphism in patients with psoriasis. Biomedical Res28, 3619–3622 (2017).

93. Lahmer Tet al., Mineralocorticoid receptor antagonism and aldosterone synthesis inhibition do not improve glomerulosclerosis and renal interstitial fibrosis in a model of chronic kidney allograft injury. Kidney Blood Press Res35, 561–567 (2012). [PubMed: 22890233]

94. Paust HJet al., The IL-23/Th17 axis contributes to renal injury in experimental glomerulonephritis. J Am Soc Nephrol20, 969–979 (2009). [PubMed: 19339380]

95. Khan SBet al., Antibody blockade of TNF-alpha reduces inflammation and scarring in experimental crescentic glomerulonephritis. Kidney Int67, 1812–1820 (2005). [PubMed: 15840028]

96. Le Hir M, Haas C, Marino M, Ryffel B, Prevention of crescentic glomerulonephritis induced by anti-glomerular membrane antibody in tumor necrosis factor-deficient mice. Lab Invest78, 1625–1631 (1998). [PubMed: 9881962]

97. Karkar AM, Smith J, Pusey CD, Prevention and treatment of experimental crescentic glomerulonephritis by blocking tumour necrosis factor-alpha. Nephrol Dial Transplant16, 518–524 (2001). [PubMed: 11239025]

98. Krebs CFet al., Autoimmune Renal Disease Is Exacerbated by S1P-Receptor-1-Dependent Intestinal Th17 Cell Migration to the Kidney. Immunity45, 1078–1092 (2016). [PubMed: 27851911]

99. Hunemorder Set al., TH1 and TH17 cells promote crescent formation in experimental autoimmune glomerulonephritis. J Pathol237, 62–71 (2015). [PubMed: 25965582]

100. Noack M, Beringer A, Miossec P, Additive or Synergistic Interactions Between IL-17A or IL-17F and TNF or IL-1beta Depend on the Cell Type. Front Immunol10, 1726 (2019). [PubMed: 31396230]

101. Griffin GKet al., IL-17 and TNF-alpha sustain neutrophil recruitment during inflammation through synergistic effects on endothelial activation. J Immunol188, 6287–6299 (2012). [PubMed: 22566565]

102. Shen Fet al., Combined Blockade of TNF-alpha and IL-17A Alleviates Progression of Collagen-Induced Arthritis without Causing Serious Infections in Mice. J Immunol202, 2017–2026 (2019). [PubMed: 30745461]

103. Gijbels K, Brocke S, Abrams JS, Steinman L, Administration of neutralizing antibodies to interleukin-6 (IL-6) reduces experimental autoimmune encephalomyelitis and is associated with elevated levels of IL-6 bioactivity in central nervous system and circulation. Mol Med1, 795–805 (1995). [PubMed: 8612202]

104. Schaeffer V, Hansen KM, Morris DR, LeBoeuf RC, Abrass CK, RNA-binding protein IGF2BP2/IMP2 is required for laminin-beta2 mRNA translation and is modulated by glucose concentration. Am J Physiol Renal Physiol303, F75–82 (2012). [PubMed: 22513850]

105. Ramani Ket al., IL-17 Receptor Signaling Negatively Regulates the Development of Tubulointerstitial Fibrosis in the Kidney. Mediators Inflamm2018, 5103672 (2018). [PubMed: 30405320]

106. Li D.-d.et al., Antibody-induced glomerulonephritis pathology is amplified by RTEC-intrinsic IL-17 signaling and restrained by the endoribonuclease Regnase-1. BioRXiv 2021/425972, (2021).

107. Ramani Ket al., Unexpected kidney-restricted role for IL-17 receptor signaling in defense against systemic Candida albicans infection. JCI Insight3, (2018).

108. Ruddy MJ, Shen F, Smith J, Sharma A, Gaffen SL, Interleukin-17 regulates expression of the CXC chemokine LIX/CXCL5 in osteoblasts: Implications for inflammation and neutrophil recruitment. J. Leukoc. Biol76, 135–144 (2004). [PubMed: 15107456]
109. Maekawa Tet al., Antagonistic effects of IL-17 and D-resolvins on endothelial Del-1 expression through a GSK-3beta-C/EBPbeta pathway. Nat Commun6, 8272 (2015). [PubMed: 26374165]
110. Song X, Qian Y, The activation and regulation of IL-17 receptor mediated signaling. Cytokine62, 175–182 (2013). [PubMed: 23557798]
111. Iwakura Y, Ishigame H, Saijo S, Nakae S, Functional specialization of interleukin-17 family members. Immunity34, 149–162 (2011). [PubMed: 21349428]
112. Hao S, Baltimore D, The stability of mRNA influences the temporal order of the induction of genes encoding inflammatory molecules. Nat Immunol10, 281–288 (2009). [PubMed: 19198593]
113. Sun SC, The non-canonical NF-kappaB pathway in immunity and inflammation. Nat Rev Immunol17, 545–558 (2017). [PubMed: 28580957]
114. Fu M, Blackshear PJ, RNA-binding proteins in immune regulation: a focus on CCCH zinc finger proteins. Nat Rev Immunol17, 130–143 (2017). [PubMed: 27990022]
115. Dai Net al., IGF2 mRNA binding protein-2 is a tumor promoter that drives cancer proliferation through its client mRNAs IGF2 and HMGA1. Elife6, (2017).
116. Conway AEet al., Enhanced CLIP Uncovers IMP Protein-RNA Targets in Human Pluripotent Stem Cells Important for Cell Adhesion and Survival. Cell Rep15, 666–679 (2016). [PubMed: 27068461]
117. Crooke ST, Witztum JL, Bennett CF, Baker BF, RNA-Targeted Therapeutics. Cell Metab27, 714–739 (2018). [PubMed: 29617640]
118. Sahin U, Kariko K, Tureci O, mRNA-based therapeutics--developing a new class of drugs. Nat Rev Drug Discov13, 759–780 (2014). [PubMed: 25233993]
119. Dobin Aet al., STAR: ultrafast universal RNA-seq aligner. Bioinformatics29, 15–21 (2013). [PubMed: 23104886]
120. Dominguez Det al., Sequence, Structure, and Context Preferences of Human RNA Binding Proteins. Mol Cell70, 854–867 e859 (2018). [PubMed: 29883606]

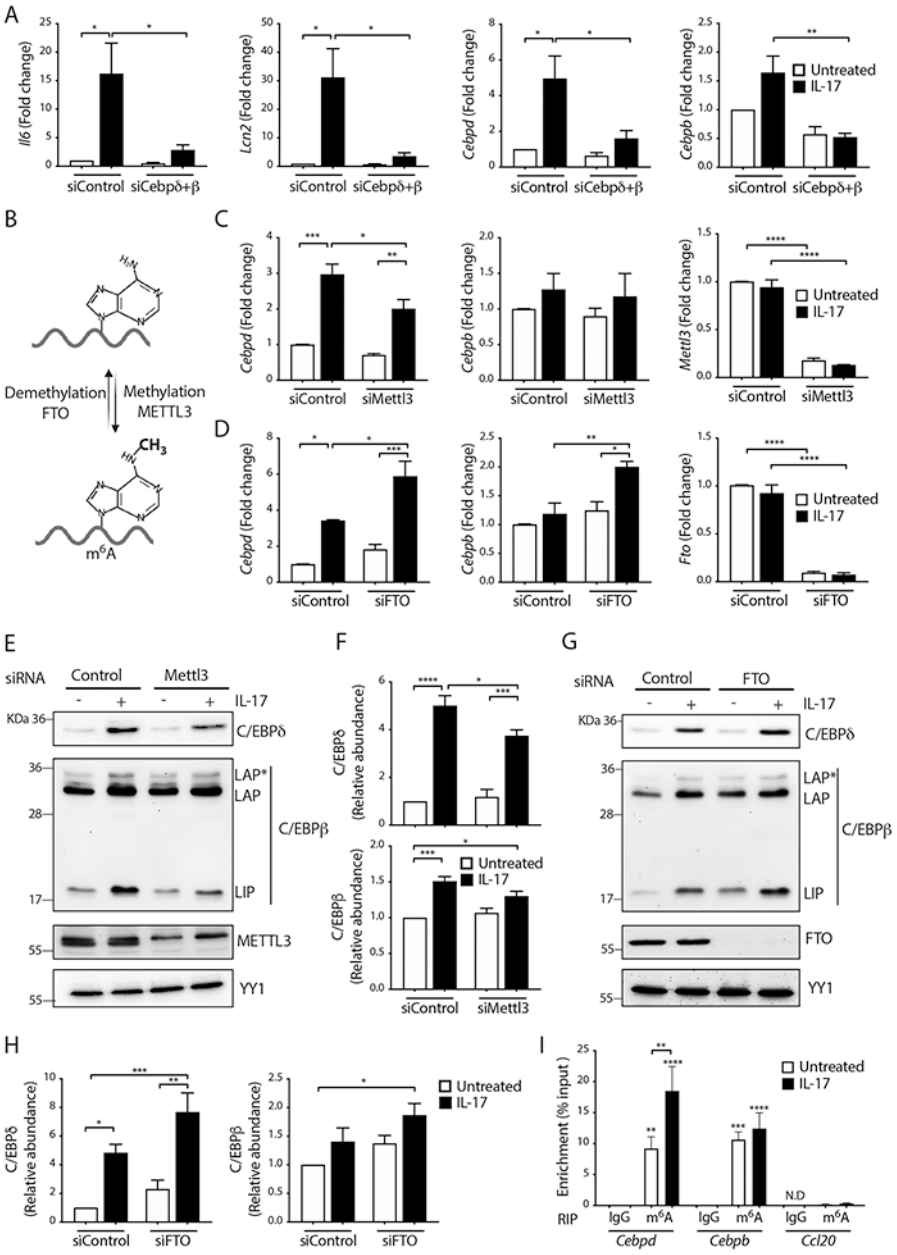

Fig 1. Cebpd and Cebpb mRNAs are subject to m^{6}A modification

(A) MEFs were transfected with siRNAs targeting *Cebpd* and *Cebpb* or control and treated ± IL-17 for 8 h. qPCR of the indicated mRNAs is shown. Data are normalized to untreated samples with control siRNA, from 3 independent experiments ± SEM. (B) Diagram of m^{6}A modification by the m^{6}A methyltransferase (writer) METTL3, and removal by the m^{6}A demethylase (eraser) FTO. (C, D) MEFs were transfected with siRNAs targeting *Mettl3* or *Fto* or non-targeting controls and treated ± IL-17 for 8 h. qPCR of the indicated mRNAs is shown. Data are normalized to untreated samples with control siRNA ± SEM, from 3 independent experiments. (E) MEFs were transfected with the indicated siRNAs and treated ± IL-17 for 6 h. C/EBPδ and C/EBPβ (isoforms LAP*, LAP and LIP (16) were assessed in nuclear extracts by immunoblotting. Blots are representative of 3-4 independent

experiments. (F) Band intensity values were quantified from immunoblots. Means ± SEM from all experiments are shown. (G) MEFs transfected with the indicated siRNAs and treated ± IL-17 for 6 h. C/EBPδ and C/EBPβ were assessed in nuclear extracts by immunoblotting. Blots are representative of 4 independent experiments. (H) Band intensity values quantified from immunoblots. Means ± SEM from pooled experiments. (I) MEFs were treated with IL-17 for 3 h and subjected to RIP with m^6A or IgG control Abs. qPCR of the indicated mRNAs is presented as % input. Data show mean ± SEM from 4 experiments. *P<0.05, **P<0.01, ***P<0.001, ****P<0.0001 by ANOVA with post hoc Tukey's test. N.D, not detected.

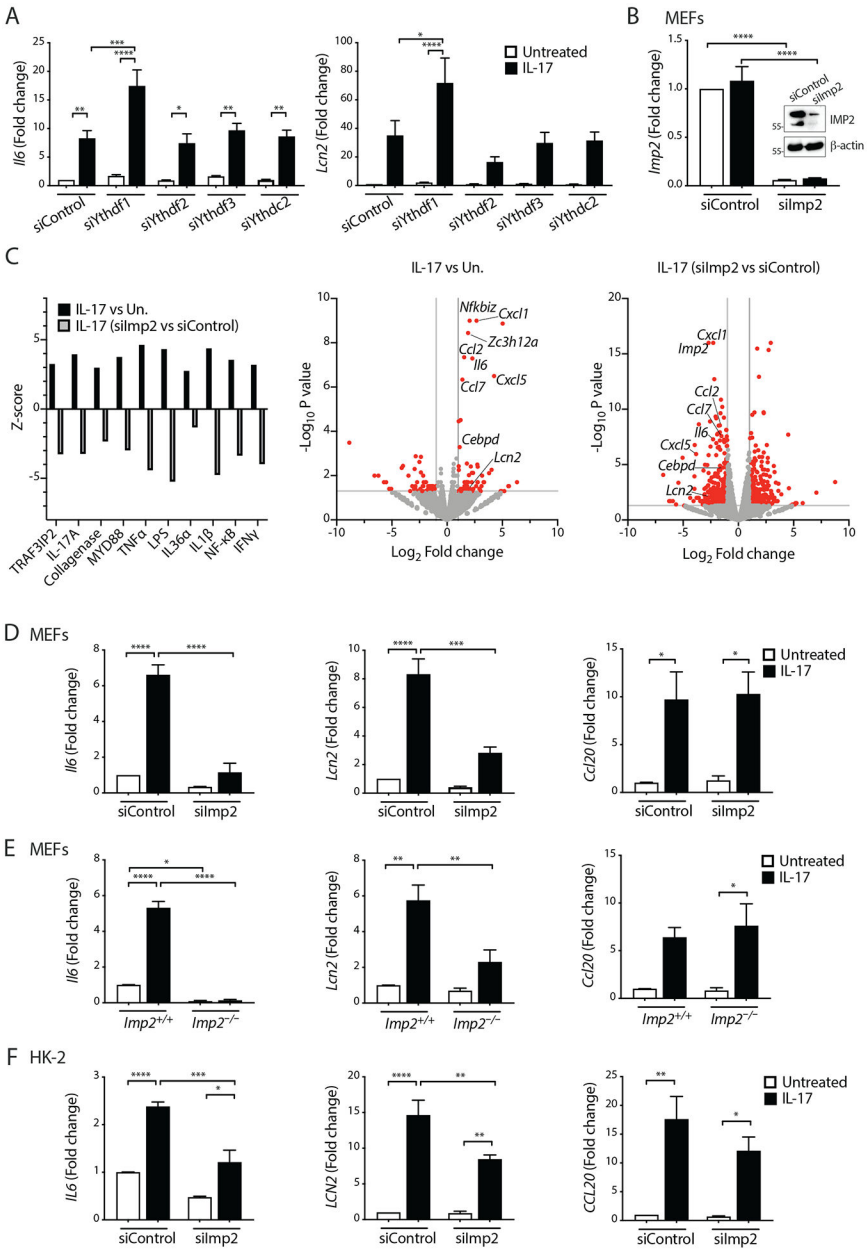

Fig. 2. IMP2 but not other m^{6}A readers promote expression of IL-17 target genes

(A) MEFs were transfected with the indicated siRNAs and treated ± IL-17 for 8 h. qPCR of the indicated mRNAs is shown. Data are normalized to untreated samples with control siRNA ± SEM, from 3 independent experiments. (B) MEFs were transfected with the indicated siRNAs. qPCR and immunoblot of IMP2 is shown. Data are normalized to untreated samples with control siRNA ± SEM, from 3 independent experiments. (C) MEFs were transfected with siRNAs targeting *Imp2* or non-targeting controls and treated ± IL-17 for 8 h. RNA-seq (n=3) was performed on the Illumina platform. Ingenuity Pathway Analysis of RNASeq showing top 10 predicted upstream regulators. Volcano plots showing the transcriptional response induced by IL-17 ± siImp2. In red are selected transcripts that were significantly changed (P value <0.05 and fold change > 2 or < −2; based on

3 experiments). (D) MEFs were transfected with siRNAs targeting *Imp2* or non-targeting control and treated ± IL-17 for 8 h. qPCR of the indicated mRNAs is shown. Data are normalized to untreated samples with control siRNA ± SEM, from 3 independent experiments. (E) $Imp2^{+/+}$ or $Imp2^{-/-}$ MEFs were treated ± IL-17 for 4 h qPCR of the indicated mRNAs is shown. Data are normalized to untreated samples with control siRNA ± SEM, 3 independent experiments. (F) HK-2 cells were transfected with siRNAs targeting *IMP2* or non-targeting control and treated ± IL-17 for 8 h. qPCR of the indicated mRNAs is shown. Data are normalized to untreated samples with control siRNA ± SEM, from 4 independent experiments *P<0.05, **P<0.01, ***P<0.001, ****P<0.0001 by ANOVA with post hoc Tukey's test.

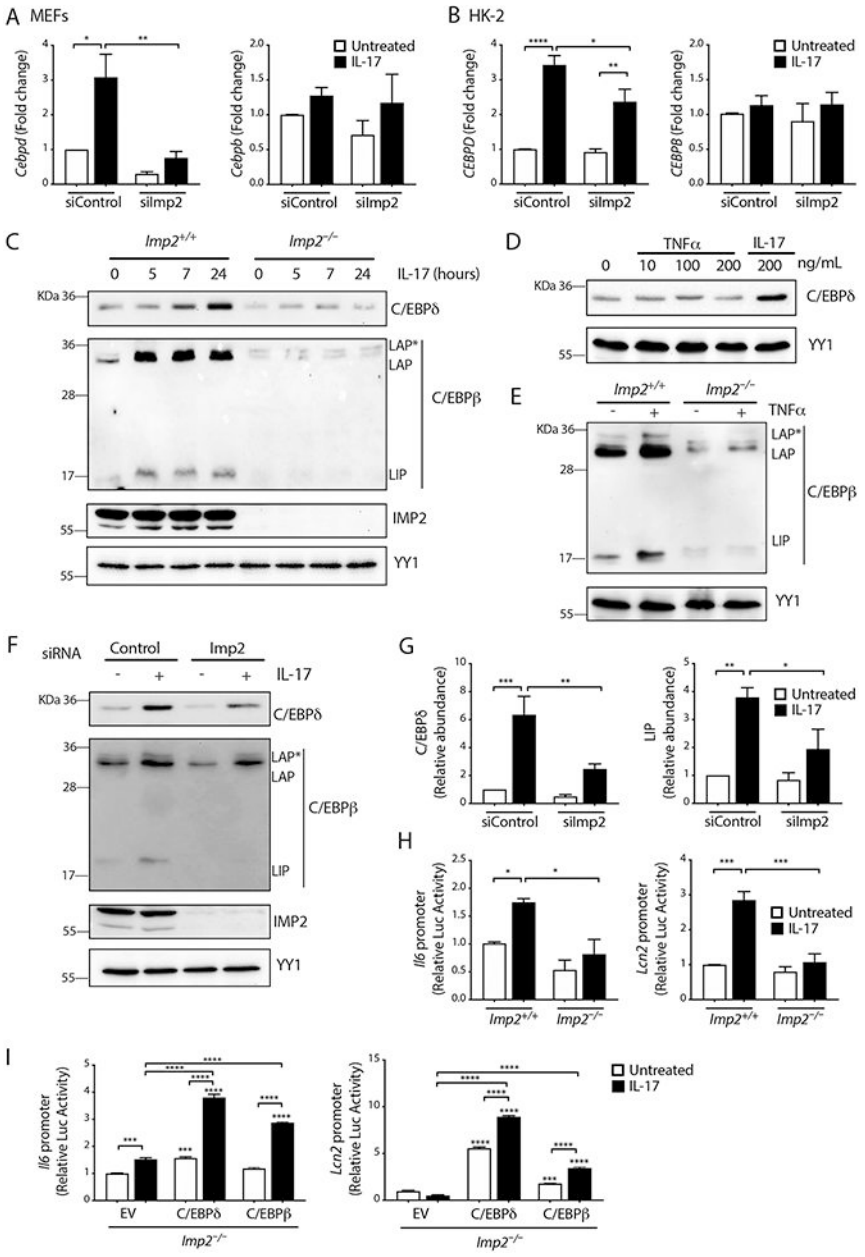

Fig 3. IMP2 regulates IL-17-induced genes via C/EBPδ and C/EBPβ

(A, B) MEFs (A) or HK-2 cells (B) transfected with pooled siRNAs targeting *Imp2* or non-targeting control and treated ± IL-17 for 8 h. qPCR of the indicated mRNAs is shown. Data are normalized to untreated samples with control siRNA ± SEM, from 3–4 independent experiments. (C) $Imp2^{+/+}$ or $Imp2^{-/-}$ MEFs treated with IL-17. C/EBPδ, C/EBPβ, IMP2 and YY1 in nuclear lysates were assessed by immunoblotting. Blots are representative of 3 experiments. (D) $Imp2^{+/+}$ MEFs treated ± indicated doses of IL-17 or TNFα. C/EBPδ and YY1 in nuclear lysates were assessed by immunoblotting. Blots are representative of 2 experiments. (E) $Imp2^{+/+}$ or $Imp2^{-/-}$ MEFs were treated ± 10 ng/ml TNFα. C/EBPβ and YY1 in nuclear lysates were assessed by immunoblotting. Blots represent 2 experiments. (F) MEFs transfected with siRNAs targeting *Imp2* or non-targeting control and treated

± IL-17 for 6 h. C/EBPδ, C/EBPβ, IMP2 and YY1 in nuclear lysates were assessed by immunoblotting. Blots are representative of 4 experiments. (G) Pooled band intensity values with mean ± SEM from 4 experiments. (H) *Imp2*$^{+/+}$ or *Imp2*$^{-/-}$ MEFs were transfected with Luc reporters driven by *Il6* or *Lcn2* promoters (6, 51). Cells were treated ± IL-17 for 8 h and Luc activity assessed. Data show fold-change relative to untreated *Imp2*$^{+/+}$ cells. (I) *Imp2*$^{-/-}$ MEFs were co-transfected with C/EBPδ or C/EBPβ (7) with *Il6*- or *Lcn2*-Luc reporters. Cells were treated ± IL-17 for 8 h and Luc activity assessed. Data show fold-change relative to EV-transfected cells. *P<0.05, **P<0.01, ***P<0.001; ****P<0.0001 by ANOVA with post hoc Tukey's test.

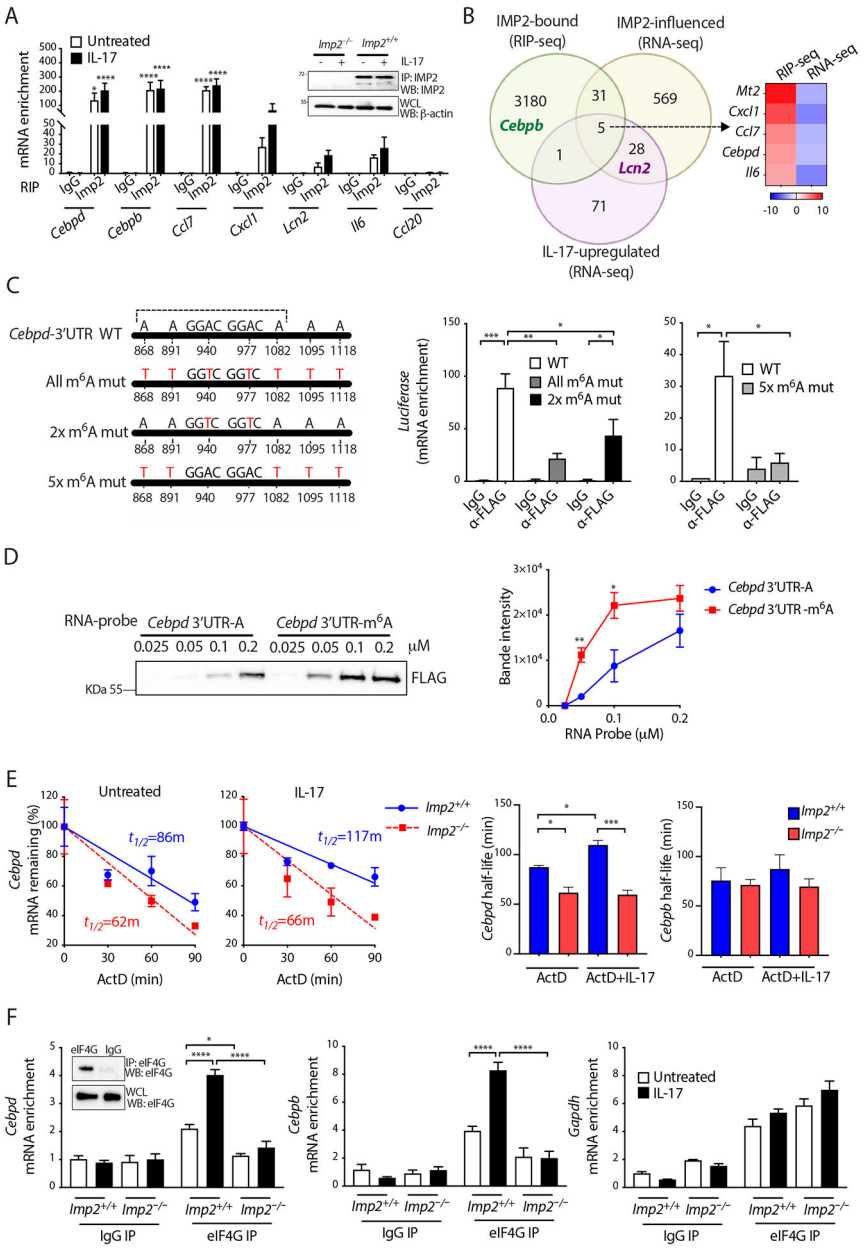

Fig 4. IMP2 binds to Cebpd and Cebpb mRNAs and mediates post-transcriptional regulation

(A) *Imp2*$^{+/+}$ MEFs were treated ± IL-17 for 3 h and subjected to RIP with anti-IMP2 or IgG Abs. qPCR of the indicated mRNAs was normalized to input. Data show mean ± SEM of 4 independent experiments. *Inset;* IMP2 immunoprecipitates from *Imp2*$^{+/+}$ and *Imp2*$^{-/-}$ MEFs was assessed by immunoblotting. (B) MEFs were treated with IL-17 for 3 h and subjected to RIP-seq with anti-IMP2 Abs. Diagram indicates the intersection between mRNAs that are IMP2-occupied based on RIPSeq compared to mRNAs that are IMP2-influenced at baseline or after IL-17 treatment. (C) Top: Diagram of *Cebpd* 3'UTR and predicted m^{6}A site mutants (sequence, fig S8). Dashed line indicates sequence in the biotinylated synthetic mRNA. Bottom: HEK293T cells were co-transfected with IMP2-FLAG and a Luc reporter fused to WT *Cebpd*-3'UTR or sequences in which putative m^{6}A sites were mutated.

Lysates were subjected to RIP with anti-FLAG Abs and *Luc* mRNA assessed by qPCR. Data are normalized to input and show mean ± SEM of 3 independent experiments. (D) Lysates from HEK293T cells transfected with FLAG-tagged IMP2 were incubated with the biotinylated mRNAs corresponding to the *Cebpd* 3' UTR (863-982, dashed line in panel C) in which indicated adenosines were m^6A-modified or unmodified. RNA pulldowns were performed with streptavidin beads. FLAG-tagged IMP2 analyzed by immunoblotting. Blots are representative of 3 experiments. Pooled band intensity values with mean ± SEM. (E) MEFs were treated with TNFα for 3 h, given actinomycin D ± IL-17 for the indicated times, and *Cebpd* assessed by qPCR. *Left:* Data normalized to time=0 (100%), representative of 3 independent experiments. *Right:* Half-life was estimated by linear regression (17). (F) MEFs were treated ± IL-17 for 3 h and subjected to RIP with anti-eIF4G Abs. mRNAs were assessed by qPCR. Data normalized to untreated $Imp2^{+/+}$ samples precipitated with IgG. Data are representative of 2 independent experiments. *Inset*; eIF4G in cytoplasmic RIP fractions from $Imp2^{+/+}$ MEFs. *P<0.05, **P<0.01, ***P<0.001, and ****P<0.0001 by ANOVA with post hoc Tukey's test or t-test.

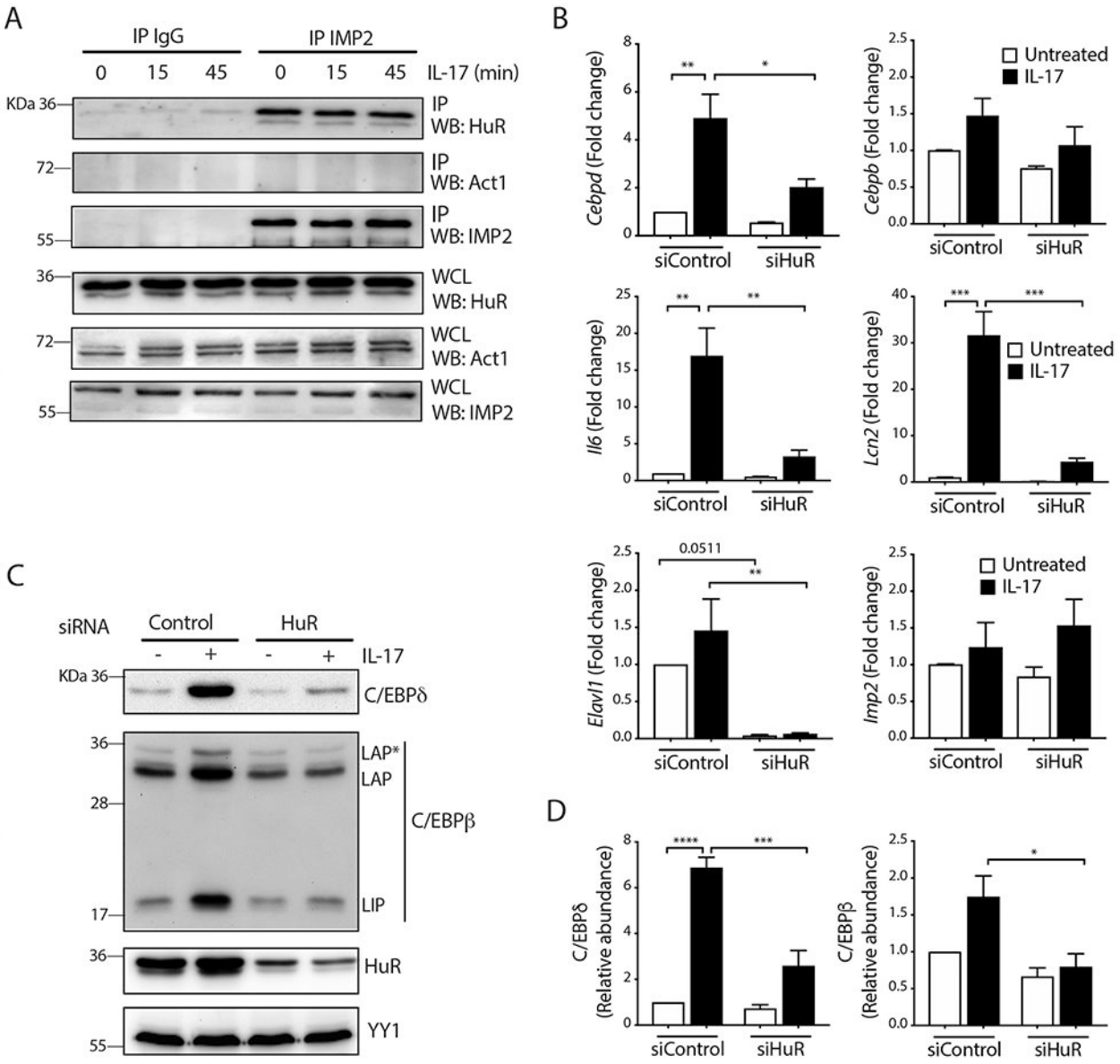

Fig 5. IMP2 forms a complex with HuR to regulate C/EBPs

(A) *Imp2*$^{+/+}$ MEFs were treated ± IL-17 and immunoprecipitated with anti-IMP2 Abs or IgG controls. Blots are representative of 2 independent experiments. (B) MEFs were transfected with pooled siRNAs targeting *HuR* (*Elavl1*) or control and treated ± IL-17 for 8 h. Data show mean ± SEM of 3 experiments normalized to untreated. (C) MEFs were transfected with siRNAs targeting *HuR* or non-targeting control and treated ± IL-17 for 6 h. C/EBPδ, C/EBPβ, HuR and YY1 were assessed by immunoblotting. Blots are representative of 3 experiments. (D) Pooled band intensity values with mean ± SEM from all experiments. *$P < 0.05$, **$P < 0.01$, ***$P < 0.001$, and ****$P < 0.0001$ by ANOVA with post hoc Tukey's test.

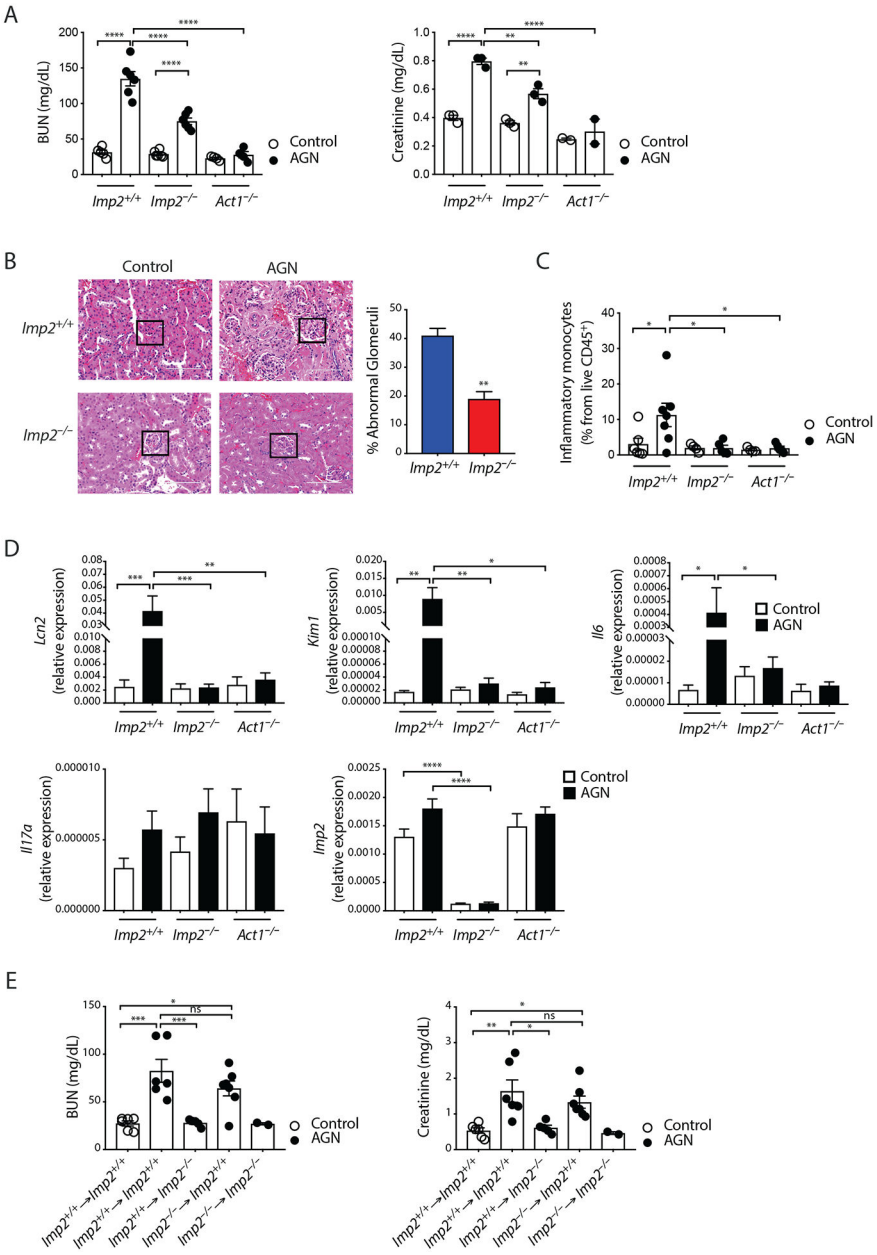

Fig 6. IMP2 deficient mice are resistant to IL-17-driven renal autoimmune inflammation

(A-B) *Imp2*$^{+/+}$, *Imp2*$^{-/-}$ and *Act1*$^{-/-}$ mice were subjected to AGN (71). Renal dysfunction was assessed at day 14 by ELISA of serum BUN and creatinine. Data pooled from 2 experiments. (B) *Left*: Representative images of H&E-stained kidney sections at day 14 of AGN (400×). *Right*: Slides were scored for abnormal glomeruli in *Imp2*$^{+/+}$ and *Imp2*$^{-/-}$ mice (n=3) at day 14 post-AGN. Bars show mean ± SEM. (C) Kidney homogenates were prepared on day 7. Live inflammatory monocytes were determined by staining for CD11b, Ly6C and Ly6G, gated on the live CD45^{+} population. Graphs show percent of live CD45^{+}CD11b^{+}Ly6C^{high}Ly6G^{-} cells. Data were pooled from 2 independent experiments. (D) The indicated mice were subjected to AGN (*Imp2*$^{+/+}$ control n=10; *Imp2*$^{+/+}$ AGN n=11, *Imp2*$^{-/-}$ control n=8, *Imp2*$^{-/-}$ AGN n=10, *Act1*$^{-/-}$ control n=6 and *Act1*$^{-/-}$ AGN n=6). Total

RNA was extracted at day 7 and subjected to qPCR. Data were pooled from 2 experiments. (E) *Imp2*$^{+/+}$ or *Imp2*$^{-/-}$ mice were lethally irradiated (900 rad) and reconstituted with BM from the indicated donor mice. After 6 weeks, mice were subjected to AGN. On day 14, BUN and creatinine levels were measured by ELISA. Data pooled from 2 experiments. *P<0.05, **P<0.01, ***P<0.001, ****P<0.0001, by ANOVA with post-hoc Tukey's test.

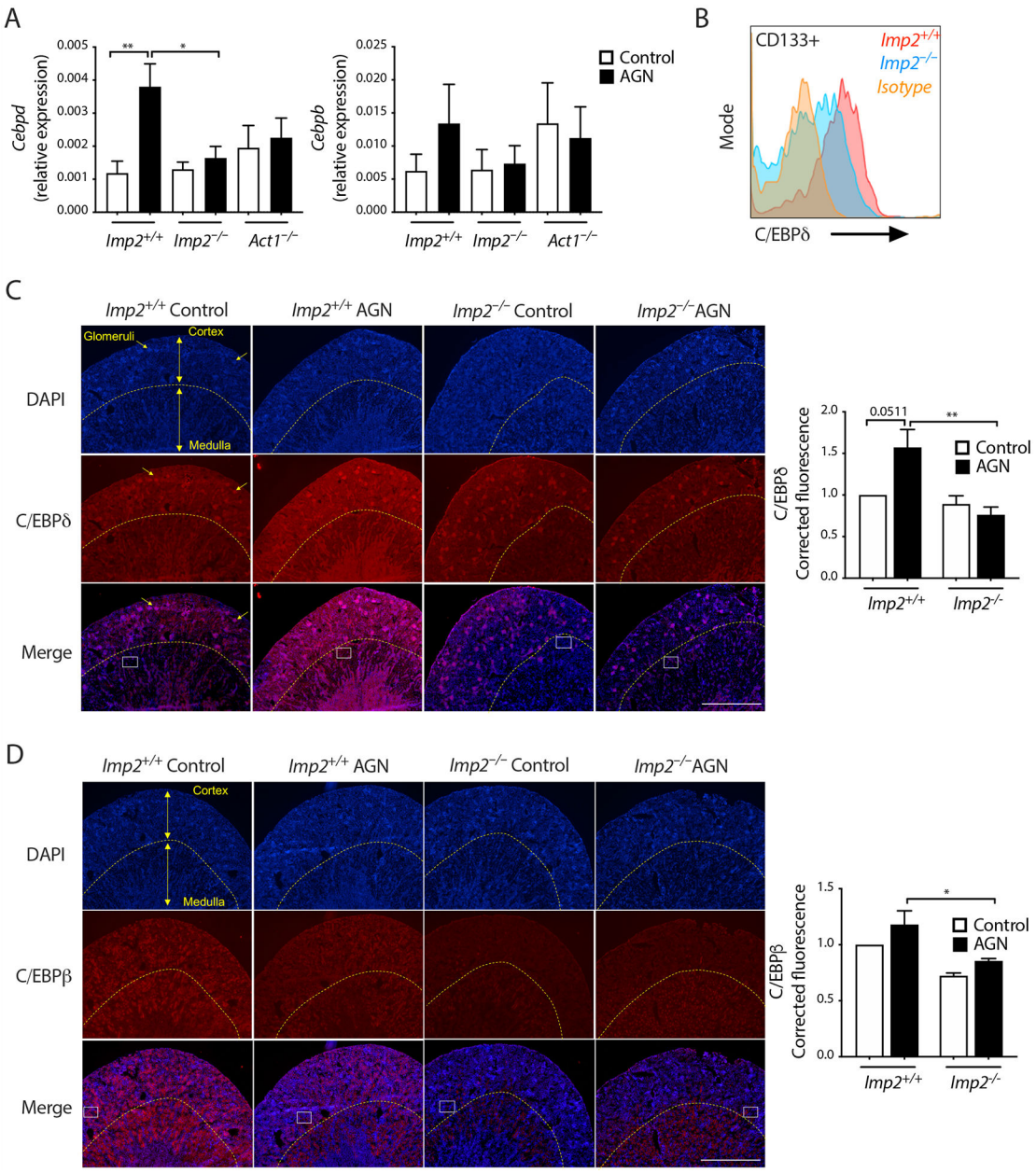

Fig. 7. Impaired C/EBP in Imp2$^{-/-}$ mice during AGN

(A) The indicated mice were subjected to AGN (*Imp2*$^{+/+}$ control n=10; *Imp2*$^{+/+}$ AGN n=11, *Imp2*$^{-/-}$ control n=8, *Imp2*$^{-/-}$ AGN n=10, *Act1*$^{-/-}$ control n=6 and *Act1*$^{-/-}$ AGN n=6). RNA at day 7 was subjected to qPCR ± SEM. (B) Kidney homogenates from the indicated mice day 7 post-AGN were stained for CD45, CD133 and intracellular C/EBPδ. Data show live CD45^{-}CD133^{+} cells. Representative FACS plot is shown. (C, D) *Left:* IF staining of C/EBPδ and C/EBPβ on day 7 post-AGN. Arrows indicate glomeruli. Cortex and medulla in a representative image are indicated. (4X). White boxes indicate sites of 40X images, fig S9. *Right:* Fluorescence intensity in non-glomerular regions of kidney was quantified by Image J, normalized to *Imp2*$^{+/+}$ control. Data are from two regions per slide and 2-3 independent

slides (2 mice). *P<0.05, **P<0.01 by ANOVA with post hoc Tukey's test. Scale bars = 1 mm.

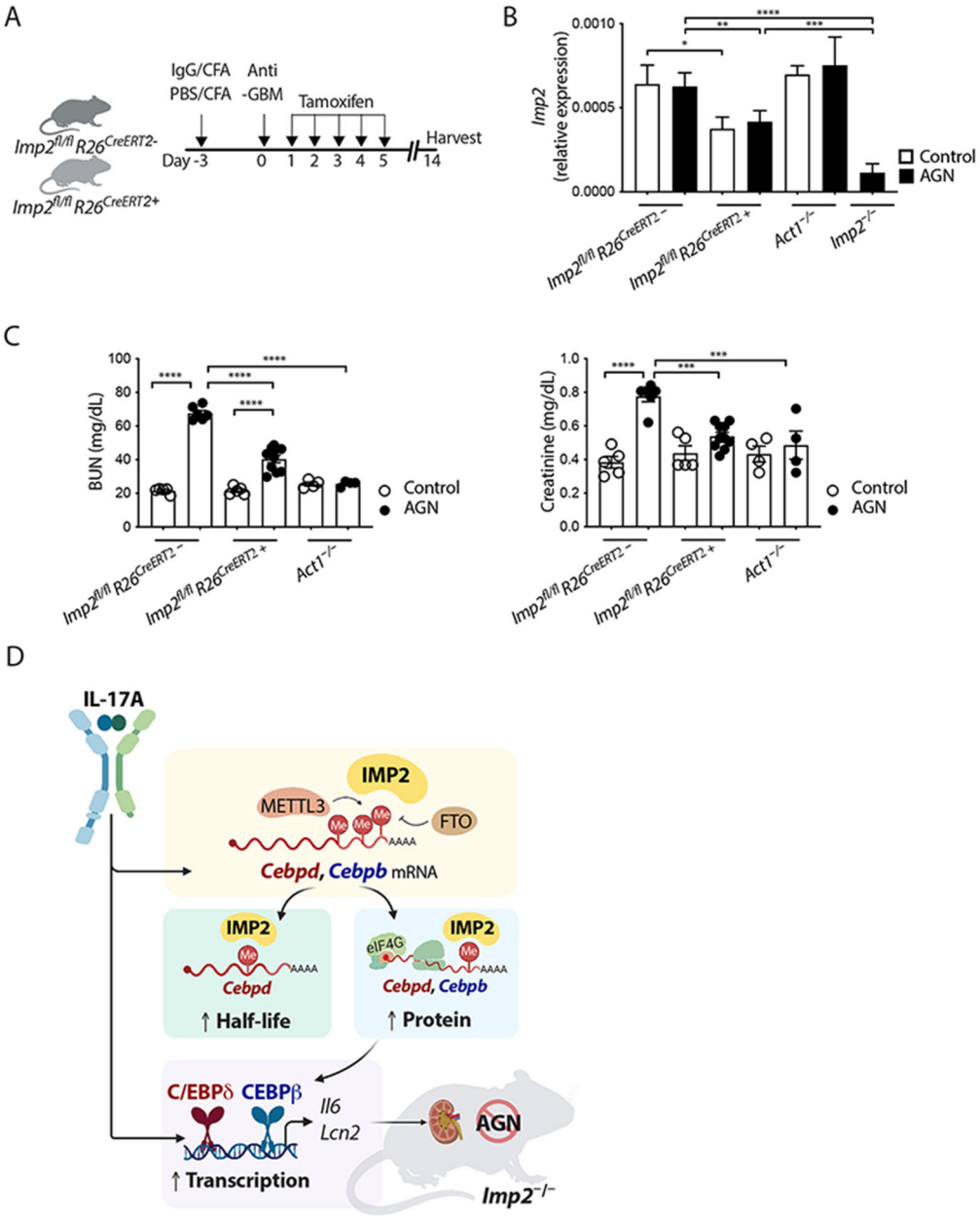

Fig. 8. Imp2 deletion post AGN induction decreased autoimmune renal dysfunction.

(A-C) Indicated mice were administered 2 mg tamoxifen (TAM) i.p. for 5 days starting day 1 after AGN induction. (B) *Imp2* was assessed by qPCR at day 14. (C) BUN and creatinine were assessed at day 14. Data pooled from 2 experiments. *P<0.05, **P<0.01, ***P<0.001, ****P<0.0001, by ANOVA with post-hoc Tukey test. (D) Model of signaling through IMP2. *Cebpb and Cebpd* transcripts are subject to m^6A modifications, which facilitate IMP2 mediated-post-transcriptional regulation. *Imp2* deficiency impaired mRNAs whose expression is dependent on C/EBPs. *Imp2*-deficient mice are resistant to IL-17-driven renal inflammation. Diagram created on Biorender.com.